Reactivity of the Mo(O)(S) Functional Group in the $[(L)Mo(O)(\mu\text{-}S)_2Mo(O)(S)]^{n-}$ Dimeric Thiomolybdate Complexes ($L = C_5H_5^-$, $n = 1$; S_4^{2-}, $n = 2$) and Implications Regarding the Function of Xanthine Oxidase. Synthesis and Structural Characterization of $[(DMF)_3Mo(O)(\mu\text{-}S)_2Mo(O)(S_2)]$, $[Ph_4P][(C_5H_5)Mo(O)(\mu\text{-}S)_2Mo(O)(S_2)]$, $[Ph_4P]_2[(S_4)Mo(O)(\mu\text{-}S)_2Mo(O)(S)]$, and $(Et_4N)_4\{[(S_4)Mo(O)(\mu\text{-}S)_2Mo(O)(S)]_2\}$

D. Coucouvanis,* A. Toupadakis, J. D. Lane, S. M. Koo, C. G. Kim, and A. Hadjikyriacou

Contribution from the Department of Chemistry, The University of Michigan, Ann Arbor, Michigan, 48109-1055. *Received December 26, 1990*

Abstract: The syntheses and structures of the diamagnetic $[(DMF)_3Mo(O)(\mu\text{-}S)_2Mo(O)(S_2)]$, I, $[Ph_4P][(C_5H_5)Mo(O)(\mu\text{-}S)_2Mo(O)(S_2)]$, IV, $(Ph_4P)_2[(S_4)Mo(O)(\mu_2\text{-}S)_2Mo(O)(S)]$, IX, and $(Et_4N)_4\{[(S_4)Mo(O)(\mu_2\text{-}S)_2Mo(O)(S)]_2\}$, X, complexes are reported. The compounds I, IV, IX, and X crystallize in the space groups *Pcab*, $P\bar{1}$, $P\bar{1}$, and $P2_1/m$, respectively. The cell dimensions for I are as follows: $a = 13.152$ (3) Å, $b = 17.554$ (5) Å, $c = 17.893$ (5) Å, $\alpha = \beta = \gamma = 90$ and $Z = 8$; for IV, $a = 11.262$ (4) Å, $b = 11.688$ (4) Å, $c = 13.188$ (4) Å, $\alpha = 102.11$ (2)°, $\beta = 91.73$ (3)°, $\gamma = 60.72$ (2)°, and $Z = 2$; for IX, $a = 10.456$ (6) Å, $b = 12.246$ (6) Å, $c = 19.785$ (7) Å, $\alpha = 100.50$ (2)°, $\beta = 78.63$ (4)°, $\gamma = 84.62$ (4)°, and $Z = 2$; and for X, $a = 9.261$ (2) Å, $b = 33.909$ (8) Å, $c = 10.082$ (2) Å, $\beta = 115.62$ (2)°, and $Z = 2$. Crystallographic data for the four structures were obtained on an automatic diffractometer employing Mo Kα radiation. The refinement of the structures by full-matrix least-squares methods was based on 1573 unique reflections ($2\theta_{max} = 40°$, all data) for I, on 3180 unique reflections ($2\theta_{max} = 45°$, $I > 3\sigma I$) for IV, on 4193 unique reflections ($2\theta_{max}$ 45°, $I > 3\sigma I$), for IX, and on 2904 unique reflections ($2\theta_{max} = 45°$, $I > 3\sigma I$) for X. Anisotropic temperature factors were used for all non-hydrogen atoms in I, IV, IX, and X. At the current stage of refinement on 208 parameters for I, 343 parameters for IV, 551 parameters for IX, and 286 parameters for X with all atoms present in the asymmetric units, $R_w = 0.039$, 0.038, 0.060, and 0.053, respectively. The structures of the complexes in I, IV, and IX contain the $[Mo_2(\mu_2\text{-}S)_2(O)_2]^{2+}$ cores with the Mo=O units in the syn configuration. The structure of X is a tetranuclear dimer of IX and contains two fused $[(S_4)Mo(O)(\mu_2\text{-}S)_2Mo(O)(S)]^{2-}$ units that share a common $Mo_2O_2(\mu_2\text{-}S)_2$ unit and are related by a crystallographic mirror plane. The four Mo=O units are all in a syn configuration. Selected structural features for I, that contains a six-coordinate Mo bound by three facially arranged DMF ligands, include the following: Mo–Mo, 2.813 (1) Å; Mo–S_b, 2.317 (3); Mo=O, 1.686 Å; $\overline{Mo\text{–}O_{DMF}} = 2.207$ (14) Å; Mo–S_b–Mo, 74.77°; S_b–Mo–S_b, 102.5°. Selected structural features for IV include the following: Mo–Mo, 2.855 (1) Å; Mo–S_b, 2.310 (4); Mo=O, 1.673 Å; $\overline{Mo\text{–}C_{cp}} = 2.380$ (9) Å; Mo–S_b–Mo, 76.32°; S_b–Mo–S_b, 101.3°. The Mo–Mo distance in IX is found at 2.896 (1) Å. In X, the Mo–Mo distance of the outer Mo–$(\mu_2\text{-}S)_2$–Mo units at 2.852 (2) Å is shorter than the Mo–Mo distance in the central Mo–$(\mu_2\text{-}S)_2$–Mo unit at 3.554 (2) Å. The long Mo–S_b bond in the central Mo–$(\mu_2\text{-}S)_2$–Mo unit in X at 2.420 Å by comparison to the Mo–S_b bonds in the outer Mo–$(\mu_2\text{-}S)_2$–Mo unit in X (2.337 Å), or the same unit in IX, (2.325 Å) underscore the weak nature of the central Mo–$(\mu_2\text{-}S)_2$–Mo unit in X. Consistent with the crystallographic results is the solution behavior of IX and X that shows dimer–tetramer equilibria for these complexes. The reaction of IV with Ph_3P affords the $[(C_5H_5)Mo(O)(\mu\text{-}S)_2Mo(O)(S)]^-$ anion that in solution exists in equilibrium with the $\{[(C_5H_5)Mo(O)(\mu\text{-}S)_2Mo(O)(S_2)]_2\}^{2-}$ tetramer. In DMF solution, at 310 K, $K_{eq} = 1 \times 10^{-3}$. The reactions of the Mo=S chromophores, in the Mo(O)(S) units of these complexes and their derivatives, with dicarbomethoxyacetylene and CS_2 are described. The possible significance of an active Mo=S functional group in enzymatic oxotransferase reactions and in the industrially important hydrodesulfurization reaction is discussed.

Introduction

The simplest among the S_x^{2-} ligands found in the thio- and oxothiomolybdate complexes is the S^{2-} ligand that exists mainly as (a) a terminal ligand in thiomolybdenyl units,[1-3] (Mo^{n+}=S, $n = 4, 5, 6$), (b) a μ_2-bridging unit in cores such as $(Mo_2S_2)^{6+}$ [1-4] and (c) a μ_3-bridging unit in $[Mo_3S_{13}]^{2-}$ [5] and in the Mo_4S_4 cores of the $[(L_3Mo)_4S_4]$ [6,7] and $[Mo_7S_8(H_2O)_{18}]^{8+}$ [8] complexes. The nucleophilicity that dominates the chemistry of the S^{2-} ligands depends on the coordination mode (a, b, or c above) and appears to be more pronounced for the terminal Mo=S sulfido ligands. In this paper we will direct our attention to the chemistry of S^{2-} terminal ligands in oxothiomolybdate complexes that contain the $Mo(S_t)(O_t)$ subunits. Previous synthetic studies have revealed the reactivity of the Mo^{n+}=S group in (a) sulfur addition reactions,[2] (b) reactions with various transition-metal ions,[9] dimeri-

(1) Coucouvanis, D.; Hadjikyriacou, A. I.; Draganjac, M.; Kanatzidis, M. G.; Ileperuma, O. *Polyhedron* **1986**, *5*, 349.
(2) Hadjikyriacou, A. I.; Coucouvanis, D. *Inorg. Chem.* **1987**, *26*, 2400.
(3) Muller, A. *Polyhedron* **1986**, *5*, 323.
(4) Harmer, M. A.; Halbert, T. R.; Pan, W.-H.; Coyle, C. L.; Cohen, S. A.; Stiefel, E. I. *Polyhedron* **1986**, *5*, 341.
(5) Muller, A.; Bhattacharyya, R. G.; Pfefferkorn, B. *Chem. Ber.* **1979**, *112*, 778.
(6) Martinez, M.; Ooi, B.-L.; Sykes, A. G. *J. Am. Chem. Soc.* **1987**, *109*, 4615.
(7) Shibahara, T.; Kuroya, H.; Matsumoto, K.; Ooi, S. *J. Am. Chem. Soc.* **1984**, *106*, 789.
(8) Shibahara, T.; Yamamoto, T.; Kanadani, H.; Kuroya, H. *J. Am. Chem. Soc.* **1987**, *109*, 3495.

0002-7863/91/1513-5271$02.50/0

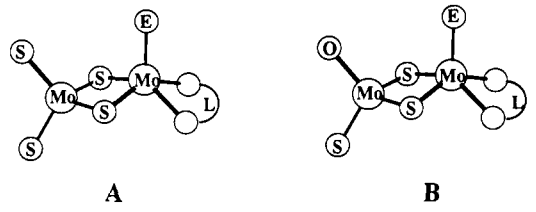

Figure 1. Schematic structures of A the $[(MoS_4)Mo(E)(L)]^{2-}$ complexes (E = S; L = S_4^{2-}, S_2^{2-};[1] E = O; L = S_4^{2-}, S_2^{2-}[2]) and B the $[(MoOS_3)Mo(E)(L)]^{2-}$ complexes.

zation reactions,[1] and (d) reactions with unsaturated electrophilic organic molecules.[1,10,11]

The addition of sulfur to terminal sulfido ligands, very likely is the end result of electrophilic attack on the Mo^{n+}=S (n = 4, 5, 6) sulfur, by the $^{+}S(S)_xS^{-}$ products of heterolytically cleaved S_8 molecules, and accounts for the synthesis of the $[(S_4)_2Mo^{IV}=E]^{2-}$ anions[12] (E = S, O) and various members of the $[Mo^{V}_2(S)_n(S_2)_{6-n}]^{2-}$[2] and $[Mo^{V}_2(O)(S)_n(S_2)_{5-n}]^{2-}$[13] series. With transition-metal ions, the thiomolybdenyl groups can serve as either electron pair donors or as a source of sulfide ions for the eventual formation of highly insoluble, thermodynamically stable, transition-metal sulfides. The former course of reactivity is represented in the multitude of heterometallic complexes where the MoS_4^{2-} anion serves as a ligand for transition-metal ions.[9] The irreversible removal of sulfide ions from Mo=S units by the formation of insoluble transition-metal sulfides allows for the introduction of non-sulfur terminal ligands in the thiomolybdate ions by metathetical reactions. An example of this reaction is available in the synthesis of the $[Mo_2O_2S_8X]^{-}$ anions[14] from the reaction of NiX_2 (X = Cl, I) with an isomeric form of the $[Mo^{VI}_2O_2S_9]^{2-}$ anion.[15]

The dimerization of Mo(V),4d[1] complexes to diamagnetic dimeric complexes with a formal Mo–Mo single bond is well-documented, and one-electron oxidations of $(L)_nMo^{IV}$—S complexes invariably lead to dimerization with formation of the very stable di-μ-sulfido, $[(L)_nMo^{V}-S]_2$ products.[16] Examples include the formation of $[(S_4)SMo^{V}=E]_2^{2-}$ from the air oxidation of $[(S_4)_2Mo^{IV}=E]^{2-}$[12] and the formation of the $[(L)_2Mo^{V}=S]_2^{2-}$ dimer[1] apparently from the oxidation of an unstable $[(L)_2Mo^{IV}=S]^{2-}$ intermediate (L = 1,2-dicarboethoxyethylene-1,2-dithiolate).

Electrophilic attack on the Mo^{n+}=S sulfur occurs in reactions of various thiomolybdates with CS_2[10] or activated alkynes, RC≡CR.[1,11] These reactions lead to the formation of perthiocarbonate or 1,2-dithiolene complexes as final products. Thus far, expected intermediates that contain vinyl sulfide or trithiocarbonate chelating ligands have not been detected in reactions with complexes that contain exclusively sulfur ligands. Apparently, the close proximity of Mo=S, Mo–S_2^{2-}, or Mo–S_4^{2-} groups to the reactive vinyl sulfide or trithiocarbonate ligands in these intermediates allows for rapid intramolecular sulfur transfer and rapid conversion to dithiolenes or perthiocarbonates. Replacement of neighboring Mo=S groups by the apparently less reactive Mo=O groups, in otherwise isostructural complexes, simplifies the reactivity patterns and eliminates some of the ambiguities inherent in the reactions of totally "sulfided" thiomolybdates. The $[(MoS_4)Mo(E)(L)]^{2-}$ complexes (E = S; L = S_4^{2-}, S_2^{2-};[2] E = O; L = S_4^{2-}, S_2^{2-}[13]) (Figure 1A) are structurally unique among the known plethora of dinuclear thio- and oxothiomolybdates. The asymmetric structures of the Mo–(μ-S)$_2$–Mo rhombic cores suggest that the mixed-valence, Mo^{IV}–Mo^{VI} state is important for the description of the electronic structure of these anions. As a consequence, these complexes (Figure 1A) in solution form only relatively weak tetranuclear dimers that exist in equilibrium with the dinuclear monomers. The isostructural $[(MoS_3O)Mo(O)(L)]^{n-}$ complexes (Figure 1B, E = O, L = S_4^{2-}, n = 2;[17] E = O, L = $C_5H_5^{-}$, n = 1[17]), that contain the MoS_3O units with Mo=O groups adjacent to the Mo=S functional group, in solution undergo similar dimerization equilibria and also are reactive toward electrophilic reagents. Indeed, the $[(MoS_3O)Mo(O)(L)]^{n-}$ complexes (Figure 1B) are ideally suited for reactivity studies of the Mo=S chromophore in the absence of other reactive, proximal, sulfido or polysulfido functional groups. Additional impetus for a study of the Mo=S chromophore within the $Mo^{VI}(O)(S)$ group is provided by the recognized importance of such a group in the oxo transferase enzymes[18] and the possible involvement of this group in the hydrodesulfurization, HDS,[19] reaction.

In this paper we report on the isolation, detailed structural characterization, and reactivities toward electrophilic reagents of the $[(DMF)_3Mo(O)(\mu\text{-}S)_2Mo(O)(S_2)]$, $[Ph_4P][(C_5H_5)Mo(O)(\mu\text{-}S)_2Mo(O)(S_2)]$, $[Ph_4P]_2[(S_4)(Mo(O)(\mu\text{-}S)_2Mo(O)(S)]$, and $(Et_4N)_4\{[(S_4)(Mo(O)(\mu\text{-}S)_2Mo(O)(S)]_2\}$ complexes. The first two of these complexes have been reported previously in a short communication[20] and a review.[21] The $\{[(S_4)(Mo(O)(\mu\text{-}S)_2Mo(O)(S)]_2\}^{4-}$ anion is a new addition to the linear, tetranuclear, chalcogenometalate complexes. The latter are quite rare and include $[W_4S_{12}]^{2-}$,[22] $Mo_4O_4S_{18}]^{2-}$,[23] and $[Nb_4Se_{22}]^{6-}$.[24]

Experimental Section

General Procedures and Techniques. The reagents and solvents in this work were used as purchased, unless otherwise stated. Anaerobic syntheses, when necessary, were carried out with a Schlenk line or in an inert atmosphere with a Vacuum-Atmospheres Dri-Lab glovebox filled with prepurified nitrogen. Acetonitrile (CH_3CN), dichloromethane (CH_2Cl_2), and diethyl ether were distilled over calcium hydride. Dimethylacetylene dicarboxylate (DMA) was distilled under reduced pressure at about 50 °C. All syntheses using oxothiomolybdate complexes were carried out under air. Those with thiomolybdate complexes were carried out anaerobically unless otherwise specified. Elemental analyses were performed by Oneida Research Services, Inc. and Galbraith Analytical Laboratories as well as by the analytical services laboratory in the department of chemistry at the University of Michigan.

Physical Methods. Visible and ultraviolet electronic spectra were obtained on a Cary 219 spectrophotometer. Infrared spectra were recorded on a Nicolet 5-DXB FT-IR spectrometer at a resolution of 4 cm^{-1} in KBr discs. Proton and carbon-13 NMR spectra were obtained on a Bruker 360 MHz Fourier transform (FT) NMR spectrometer with a

(9) (a) Coucouvanis, D.; Simhon, E. D.; Baenziger, N. C. *J. Am. Chem. Soc.* **1980**, *102*, 6644. (b) McDonald, J. W.; Friesen, G. D.; Newton, W. E. *Inorg. Chim. Acta* **1980**, *46*, L79. (c) Muller, A.; Hellmann, W.; Romer, C.; Romer, M.; Bogge, H.; Jostes, R.; Schimanski, U. *Inorg. Chim. Acta* **1984**, *83*, L75. (d) Pan, W.-H.; McKenna, S. T.; Chianelli, R. R.; Halbert, T. R.; Hutchings, L. L.; Stiefel, E. I. *Inorg. Chim. Acta* **1985**, *97*, L17. (e) Muller, A.; Diemann, F.; Jostes, R.; Bogge, H. *Angew. Chem., Int. Ed. Engl.* **1981**, *20*, 934. (f) Callahan, K. P.; Piliero, P. A. *Inorg. Chem.* **1980**, *19*, 2609. (g) Coucouvanis, D.; Stremple, P.; Simhon, E. D.; Swenson, D.; Baenziger, N. C.; Draganjac, M.; Chan, L. T.; Simopoulos, A.; Papaefthymiou, V.; Kostikas, A.; Petrouleas, V. *Inorg. Chem.* **1983**, *22*, 293–308. (h) Coucouvanis, D.; Baenziger, N. C.; Simhon, E. D.; Stremple, P.; Swenson, D.; Kostikas, A.; Simopoulos, A.; Petrouleas, V.; Papaefthymiou, V. *J. Am. Chem. Soc.* **1980**, *102*, 1730. (i) Coucouvanis, D.; Simhon, E. D.; Stremple, P.; Ryan, M.; Swenson, D.; Baenziger, N. C.; Simopoulos, A.; Papaefthymiou, V.; Kostikas, A.; Petrouleas, V. *Inorg. Chem.* **1984**, *23*, 741–749. (j) Coucouvanis, D. *Acc. Chem. Res.* **1981**, *14*, 201.

(10) (a) Coucouvanis, D.; Draganjac, M. *J. Am. Chem. Soc.* **1982**, *104*, 6820. (b) Coucouvanis, D.; Hadjikyriacou, A.; Toupadakis, A.; Koo, S.-M.; Ileperuma, O.; Draganjac, M.; Salifoglou, A. *Inorg. Chem.* **1991**, *30*, 754–767.

(11) (a) Draganjac, M.; Coucouvanis, D. *J. Am. Chem. Soc.* **1983**, *105*, 139. (b) Hadjikyriacou, A. Ph.D. Thesis, University of Michigan, 1988.

(12) Draganjac, M.; Simhon, E.; Chan, L. T.; Kanatzidis, M.; Baenziger, N. C.; Coucouvanis, D. *Inorg. Chem.* **1982**, *21*, 3321.

(13) Coucouvanis, D.; Koo, S.-M. *Inorg. Chem.* **1989**, *28*, 2.

(14) Hadjikyriacou, A. I.; Coucouvanis, D. *Inorg. Chem.* **1989**, *28*, 2169.

(15) Coucouvanis, D.; Hadjikyriacou, A. I. *Inorg. Chem.* **1987**, *26*, 1.

(16) Bunzey, G.; Enemark, J. H. *Inorg. Chem.* **1978**, *17*, 682.

(17) Toupadakis, A. Ph.D. Thesis, University of Michigan, 1990.

(18) Holm, R. H. *Coord. Chem. Rev.* **1990**, *100*, 183–221.

(19) (a) Massoth, F. E. *Adv. Catal.* **1978**, *27*, 265. (b) Topsoe, J.; Clausen, B. S. *Catal. Rev. Sci. Engl.* **1984**, *26*, 395. (c) Weisser, O.; Landa, S. *Sulfide Catalysts: Their Properties and Applications*; Pergamon Press: London, 1973.

(20) Coucouvanis, D.; Toupadakis, A.; Hadjikyriacou, A. *Inorg. Chem.* **1988**, *27*, 3272.

(21) Coucouvanis, D.; Toupadakis, A.; Koo, S.-M.; Hadjikyriacou, A. *Polyhedron* **1989**, *8*, 1705–1716.

(22) Secheresse, F.; Lefebvre, J.; Daran, J. C.; Yeannin, Y. *Inorg. Chem.* **1982**, *21*, 1311–1314.

(23) Hadjikyriacou, A. I.; Coucouvanis, D. *Inorg. Chem.* **1989**, *28*, 2169–2177.

(24) Schreiner, S.; Aleandri, L. E.; Kang, D.; Ibers, J. A. *Inorg. Chem.* **1989**, *28*, 392.

superconducting magnet. Tetramethylsilane ($(CH_3)_4Si$) was used as an internal standard. Negative ion FAB mass spectra were taken in 3-nitrobenzyl alcohol or in Magic Bullet (1:3 mixture of dithioerythritol and dithiothreitol) by using a VG Analytical 70-250-S spectrometer equipped with a Xenon gun, operated at 8 KV and 1 mA.

Synthesis. (η^2-Disulfido)(trisdimethylformamide)-*syn*-bis(μ-sulfido)-bis(oxomolybdate(V)), *syn*-[[(η^2-S_2)Mo(O)(μ-S)$_2$Mo(O)(DMF)$_3$]], I. To a solution of $(Et_4N)_2[(\eta^2\text{-}S_2)Mo(O)(\mu\text{-}S)_2Mo(O)(\eta^2\text{-}S_4)]$ (5 g, 6.75 mmol)[20] in 150 mL of DMF (Aldrich 99%, used as purchased) was added slowly (~3 min) with vigorous stirring a solution of iodine (1.71 g, 6.75 mmol) in 50 mL of DMF. After stirring for an additional 30 min, 250 mL of diethyl ether was added to precipitate the Et_4NI byproduct. The resulting suspension was allowed to settle for 10 min and then was filtered. To the filtrate was added 450 mL of ether, and the suspension was placed in the refrigerator for ~1 h. The precipitated orange powder was filtered, and after drying in vacuo was redissolved in 250 mL of dimethylformamide, DMF, with gentle heating. To the solution was added ether (~350 mL), until the clear red solution became cloudy. At this point an additional limited amount of ether was added until precipitation occurred. The small amount of flocculent precipitate that formed was filtered off, and to the filtrate was added an additional 400 mL of ether carefully so as not to disturb the interface. After standing at 5 °C for ~12 h the mixture was agitated and again allowed to stand at 5 °C for an additional 6 h. The product was isolated by filtration as an orange microcrystalline solid in 85% yield: FT-IR (KBr pellet, cm^{-1}) νC=O, DMF, 1641 (v s), 1657 (v s); νMo=O, 954 (s) and 948 (s); ν, η^2-S_2, 527 (m); νMo-S_b, 469 (m). Anal. Calcd for $C_9H_{21}N_3Mo_2S_4O_5$ (fw = 571.4): C, 18.92; H, 3.70; N, 7.35; Mo, 33.58; S, 22.44. Found: C, 19.55; H, 3.70; N, 7.43; Mo, 32.37; S, 21.70. The stoichiometry of this compound also was verified by a single-crystal X-ray structure determination. The powder pattern calculated on the basis of the single-crystal data was found to be very nearly identical with that obtained for the bulk of the compound.

(Hexakisdimethylformamide)-*syn*-bis(μ-sulfido)bis(oxomolybdenum-(V)) Diiodide, *syn*-[(DMF)$_3$Mo(O)(μ-S)$_2$Mo(O)(DMF)$_3$][I]$_2$, II. To a solution of $(Et_4N)_2[(\eta^2\text{-}S_2)Mo(O)(\mu\text{-}S)_2Mo(O)(\eta^2\text{-}S_4)]$,[20] (3 g, 4.05 mmol) in 50 mL of DMF, was added with stirring a solution of iodine (2.05 g, 8.1 mmol) in 10 mL of DMF, and stirring was continued for 15 min. At this stage, 100 mL of diethyl ether was added, and the suspension was allowed to stand for 10 min. Following filtration, ether was added to the dark solution (100 mL). Upon cooling to -10 °C for 12 h a dark film formed on the sides of the container. The dark mother liquor was decanted, and the film was dissolved in 100 mL of DMF. Upon addition of 200 mL of ether, an orange crystalline hygroscopic solid, 3.18 g, 80% yield, was obtained: FT-IR (KBr pellet, cm^{-1}) νC=O, DMF, 1647 (v s), 1664 (v s), νMo=O, 928 (m) and 947 (s), νMo-S_b, 474 (m); UV-vis (DMF solution, 10^{-3} M, nm) 358 (sh), 300 (sh), 276. Anal. Calcd for $C_{18}H_{42}N_6Mo_2S_2I_2O_8$ (fw = 980): C, 22.00; H, 4.28; N, 8.57; Mo, 19.59. Found: C, 21.8; H, 4.50; N, 8.24; Mo, 18.9.

Tetraethylammonium (η^2-Disulfido)(η^5-cyclopentadienido)-*syn*-bis(μ-sulfido)bis(oxomolybdate(V)), [Et$_4$N]-*syn*-[(η^2-S_2)Mo(O)(μ-S)$_2$Mo-(O)(η^5-C_5H_5)], III. An amount of I (2.8 g, 4.9 mmol) was added to 50 mL of dry degassed DMF under strictly anaerobic conditions. An orange suspension was obtained, and it was stirred for a few minutes. While stirring vigorously, a solution of NaCp in THF (2.5 mL, 5 mmol, Aldrich 2.0 M in THF) was added with a syringe through a septum. Immediately, a clear orange solution was obtained. To this solution, a solution of $Et_4NCl{\cdot}xH_2O$ (1.3 g, Aldrich) in a minimum amount of DMF was added, and the resulting solution was stirred for 1 min. To this solution was added 100 mL of diethyl ether. After standing for 10 min, the cloudy mixture was filtered, and to the resulting clear orange solution was added diethyl ether (~350 mL). Upon standing at -10 °C an orange solid formed, was isolated, and washed with small portions of Et_2O, isopropyl alcohol, H_2O, isopropyl alcohol, and Et_2O. After drying, the orange solid was dissolved in 70 mL of CH_3CN, and to the clear orange solution was added 130 mL of diethyl ether. The solution was agitated for ~10 min and then filtered. To the filtrate an additional 300 mL of ether was added. Upon standing at -10 °C for ~12 h an orange crystalline product formed that was isolated, washed with ether, and dried: yield, 1.92 g or 72%. FT-IR (CsI pellet, cm^{-1}) νMo=O, 909 (m) and 948 (s), νMo-S_b, 462 (m), νCp, 801 (s), 3096 (m); UV-vis (DMF solution, 5×10^{-4} M, nm) 310, 470; FAB$^-$ in magic bullet; 417 = P - Et_4N^+ = P$^-$, 369 = P$^-$ - S - [O], 570 = P$^-$ + matrix, 401 = P$^-$ - [O], 352 = P$^-$ - Cp, 538 = 570 - S, 385 = P$^-$ - S, 337 = P$^-$ - [O] - 2S, 506 = 570 - 2S. Anal. Calcd for $C_{13}H_{25}NMo_2S_4O_2$ (fw = 547.4): C, 28.52; H, 4.60; N, 2.56. Found: C, 28.59; H, 4.60; N, 2.74.

[Ph$_4$P]-*syn*-[(η^2-S_2)Mo(O)(μ-S)$_2$Mo(O)(η^5-C_5H_5)], IV. This compound is prepared in the same way as the Et_4N salt, III, by using Ph_4PCl instead of Et_4NCl. The product is isolated as orange crystals in 70% yield. FAB$^+$ in 3-nitrobenzyl alcohol: 339 = Ph_4P^+, 262 = Ph_4P^+ - Ph. FAB$^-$ in 3-nitrobenzyl alcohol: 417 = P - Ph_4P^+ = P$^-$, 385 = P$^-$ - S, 369 = P$^-$ - S - [O]. Anal. Calcd for $C_{29}H_{25}PMo_2S_4O_2$ (fw = 756.6): C, 46.04; H, 3.33; P, 4.09; Mo, 25.36; S, 16.95. Found: C, 46.07; H, 3.21; P, 4.23; Mo, 24.68; S, 17.02. Orange single crystals of the salt were obtained by vapor diffusion with the CH_3CN/Et_2O system. The stoichiometry of this compound was verified by a single-crystal X-ray structure determination.

Bis(tetraethylammonium) Bis(η^5-cyclopentadienido)hexakis(μ-sulfido)tetrakis(oxomolybdate(V)), [Et$_4$N]$_2$[*syn*-[(S)Mo(O)(μ-S)$_2$Mo-(O)(η^5-C_5H_5)]]$_2$, V. To a solution of [Et$_4$N]-*syn*-[(η^2-S_2)Mo(O)(μ-$S)_2$Mo(O)(η^5-C_5H_5)], III, (0.5 g, 0.91 mmol) in 10 mL of DMF was added slowly a solution of Ph_3P (0.27 g, 1.03 mmol) in 10 mL of DMF. The clear orange solution soon turned to red (~2 min) and was stirred for an additional 40 min. Filtration with a fine porosity fritted funnel gave a clear solution, which was then flooded with about 300 mL of diethyl ether. The precipitate that formed after ca. an hour was filtered and washed with toluene and ether. The yield was 0.4 g, 85%. The crude product can be recrystallized from a CH_3CN/Et_2O mixture: FT-IR (KBr pellet, cm^{-1}) νMo=O, 903 (s), 914 (m), 930 (s); νMo-S_b, 464 (m); νCp, 805 (s), 813 (s), 3081 (w); UV-vis (DMF solution, 10^{-3} M, nm) 320, 270 (sh); ^{1}H NMR (ppm from TMS) in DMSO-d_6, δ = 6.023 (major), δ = 6.197 (minor); in CD_3CN, δ = 6.036 (major), δ = 6.175 (minor). Anal. Calcd for $C_{26}H_{50}N_2Mo_4S_6O_4$ (fw = 1030.8): C, 30.29; H, 4.89; N, 2.72; Mo, 37.23; S, 18.66. Found: C, 29.45; H, 5.19; N, 2.48; Mo, 36.4; S, 18.94.

Tetraethylammonium (η^2-Trithiocarbonato)(η^5-cyclopentadienido)-*syn*-bis(μ-sulfido)bis(oxomolybdate(V)), [Et$_4$N]-*syn*-[(CS_3)Mo(O)(μ-S)$_2$Mo(O)(η^5-C_5H_5)], VI. Method A. To a clear orange solution of [Et$_4$N]-*syn*-[(η^2-S_2)Mo(O)(μ-S)$_2$Mo(O)(η^5-C_5H_5)], III, (0.1 g) in 20 mL of CH_3CN, a large excess of CS_2 (10 mL) was added. The solution turned to a yellow color, and the two-phase system thus formed was stirred for 1 h. At this stage ether was added until the single liquid phase that was obtained showed signs of incipient nucleation. The cloudy solution was cooled to -10 °C for ~12 h and deposited a yellow-orange microcrystalline solid. This product showed characteristic C=S vibrations for the perthiocarbonate ligand at 994 (s) and 982 (m) cm^{-1} and for the trithiocarbonate ligand at 1052 (m) cm^{-1}. This solid was dissolved in a minimum amount of CH_3CN, and an excess of Ph_3P was added. A yellow film formed upon the addition of diethyl ether. The supernatant was discarded, and the film was washed with toluene and then was redissolved in CH_3CN. Addition of ether to incipient crystallization afforded upon standing the microcrystalline product in 90% yield. FT-IR (KBr pellet, cm^{-1}) νMo=O, 911 (m), 951 (s); νMo-S_b, 466 (w); νC=S, 1052 (vs); νCp, 808 (m), 820 (m); UV-vis (DMF solution, 10^{-3} M, nm) 313 (sh), 298 (sh), 270 (sh); ^{1}H NMR (ppm from TMS) in CD_3CN, a singlet δ = 6.29 ppm. Anal. Calcd for $C_{14}H_{25}NMo_2S_5O_2$ (fw = 591.5): C, 28.42; H, 4.26; N, 2.37. Found: C, 28.64; H, 4.38; N, 2.37.

Method B. To a suspension of V (0.1 g) in 50 mL of CH_3CN was added an excess of CS_2. A yellow solution was obtained instantly. Addition of ether to this solution afforded a yellow precipitate that was recrystallized from a CH_3CN mixture to give a yellow microcrystalline product in nearly quantitative yield. The ^{1}H NMR and FT-IR spectra of this compound were found to be identical with those recorded to a sample made by method A.

Tetraethylammonium (η^1-(*S*):η^1-(*C*)-(1,2-Dicarbomethoxyvinyl)disulfido)(η^5-cyclopentadienido)-*syn*-bis(μ-sulfido)bis(oxomolybdate(V)), [Et$_4$N]-*syn*-[(η^1-S,η^1-C-$S_2C_2(CO_2CH_3)_2$)Mo(O)(μ-S)$_2$Mo(O)(η^5-C_5H_5)], VII. An amount of III (1 g, 1.83 mmol) was dissolved in 40 mL of dry degassed acetonitrile under strictly anaerobic conditions. To the clear orange solution freshly distilled DMA (0.25 mL, 2 mmol) was added dropwise with stirring. After stirring for 30 min, 200 mL of ether was added to the yellow brown solution. The resulting yellow suspension was allowed to stand at -10 °C for 12 h. At this stage the mother liquor was decanted, and the yellow, microcrystalline powder product was dissolved in the minimum required amount of an acetone/acetonitrile 1:1 mixture. To the solution was added ether until a flocculent solid stopped forming. After filtration, a large excess of ether was added to the filtrate (~250 mL), and the solution was allowed to stand at -10 °C for 12 h. The yellow solid that formed was isolated, washed with ether, and dried in air: yield 75%; FT-IR (KBr pellet, cm^{-1}) νMo=O, 906 (m), 944 (s), νMo-S_b, 464 (w), νC=O, 1694 (s), 1720 (s); UV-vis (CH_3CN solution, 10^{-3} M, nm) 462 (br sh), 395 (br sh), 298 (sh), 264 (sh), 230 (sh); ^{1}H NMR (ppm from TMS) in CD_3CN, a singlet δ = 6.160 ppm (5 H) and two single resonances from the OCH_3 groups at δ = 3.751 ppm (3 H) and δ = 3.846 ppm (3 H); FAB in magic bullet, 559 = P - Et_4N^+ = P$^-$, 527 = P$^-$ - S, 417 = P$^-$ - DMA). Anal. Calcd for $C_{19}H_{31}NMo_2S_4O_6$ (fw = 689.6): C, 33.09; H, 4.53; N, 2.03. Found: C, 33.11; H, 4.58; N, 1.98.

Bis(tetraphenylphosphonium) (η^2-Disulfido)(η^2-tetrasulfido)-*syn*-bis-(μ-sulfido)bis(oxomolybdate(V)), [Ph$_4$P]$_2$-*syn*-[(η^2-S_2)Mo(O)(μ-S)$_2$Mo-

(O)(η^2-S_4)], VIII. To a solution of *syn*-{[(DMF)$_3$Mo(O)(μ-S)$_2$Mo(O)(DMF)$_3$] was added II (0.85 g, 0.867 mmol) in 20 mL of dry, degassed DMF via a cannula to a solution of Li_2S_4. This solution was obtained by the reaction of lithium triethylborohydride (Super-Hydride) 1 M solution in THF (3.47 mL, 3.47 mmol) with elemental sulfur (0.221 g, 6.93 mmol) under strictly anaerobic conditions. After stirring for 20 min, Ph_4PCl (0.65 g, 1.73 mmol) was added to the dark green solution. Addition of Et_2O instantly changed the green solution to orange and finally an orange oil formed. This was washed with Et_2O, isopropyl alcohol, H_2O, isopropyl alcohol, and Et_2O. The solid was redissolved in CH_3CN and reprecipitated with Et_2O. Again, the solid obtained was washed and recrystallized in the same way to finally obtain the product as an orange microcrystalline solid in analytically pure form: FT-IR (KBr pellet, cm^{-1}) νMo=O, 932 (s), 950 (m), νMo–S_b, 460 (w), νMo=η^2-S_4, 420 (w); UV–vis (DMF solution, 10^{-3} M, nm) 462 (sh), 360 (sh), 296 (sh). Anal. Calcd for $C_{48}H_{40}P_2Mo_2S_8O_2$ (fw = 1159.2): C, 49.74; H, 3.48; P, 5.34; Mo, 16.55; S, 22.13. Found: C, 49.38; H, 3.27; P, 5.68; Mo, 16.43; S, 22.00.

Bis(tetraphenylphosphonium) (Sulfido)(η^2-tetrasulfido)-bis(*syn*-bis(μ-sulfido)bis(oxomolybdate(V)), [Ph_4P]$_2$-*syn*-[(S)Mo(O)(μ-S)$_2$Mo(O)(η^2-S_4)], IX. An amount of VIII (1.04 g, 0.897 mmol) and Ph_3P (2.35 g, 8.97 mmol) was dissolved in 60 mL of CH_3CN. The clear red solution that formed was stirred at ambient temperature for 21 h. At this time 200 mL of Et_2O was added to the clear red solution, and the mixture was allowed to stand at −10 °C for several hours. The cloudy orange mother liquor was decanted, and the crystalline solid was washed in sequence with Et_2O, toluene, and Et_2O, and then it was recrystallized from CH_3CN/Et_2O. The product was isolated as red crystals, 0.7 g, 70% yield: FT-IR (KBr pellet, cm^{-1}) νMo=O, 890 (m), 943 (m), νMo–S_b, 465 (mw), νMo=S_t, 494 (m); UV–vis (DMF solution, 10^{-3} M, nm) 352, 276 (sh), 262 (sh). Anal. Calcd for $C_{48}H_{40}P_2Mo_2S_7O_2$ (fw = 1127.1): C, 51.15; H, 3.58; P, 5.50; Mo, 17.02; S, 19.91. Found: C, 51.42; H, 3.54; P, 5.58; Mo, 16.68; S, 19.68.

Tetrakis(tetraethylammonium) Bis(η^2-tetrasulfido)hexakis(μ-sulfido)tetrakis(oxomolybdate(V)), [Et_4N]$_4$[*syn*-[(S)Mo(O)(μ-S)$_2$Mo(O)(η^2-S_4)]]$_2$, X. An amount of $(Et_4N)_2$[(η^2-S_2)Mo(O)(μ-S)$_2$Mo(O)(η^2-S_4)][20] (5 g, 6.75 mmol) and Ph_3P (2.00 g, 7.63 mmol) was dissolved in 100 mL of DMF, and the solution was stirred for ca. 10 h. To the solution was added 400 mL of ether, and the suspension was allowed to stand at −10 °C for 12 h. The yellow mother liquor was decanted, and about 300 mL of CH_3CN was added to dissolve the solid. After filtration, 200 mL of ether was added, and the mixture was allowed to stand at −10 °C for several hours. The precipitated orange crystalline solid was filtered and washed with ether, 3 g, 63% yield: FT-IR (KBr pellet, cm^{-1}) νMo=O, 938 (s), νMo–S_b, 460 (m), νMo–S_4, 410 (w), Mo=S_b, 492 (w); UV–vis (DMF solution, 10^{-3} M, nm) 390 (sh), 306 (sh); FAB^- in magic bullet 1222 = P − 2Et_4N^+ + H^+ + 2[S]; 1126 = P − 2Et_4N^+ + H^+ − [S]; 997 = P − 3Et_4N^+ + 2H^+ − [S]; 867 = P − 4Et_4N^+ + 3H^+ − [S]; 835 = P − 4Et_4N^+ + 3H^+ − 2[S]. Anal. Calcd for $C_{32}H_{80}N_4Mo_4S_{14}O_4$ (fw = 1417.6): C, 27.11; H, 5.69; N, 3.95; Mo, 27.07; S, 31.66. Found: C, 27.10; H, 5.38; N, 3.87; Mo, 27.00; S, 30.05.

Bis(tetraphenylphosphonium) (η^2-Trithiocarbonato)(η^2-perthiocarbonato)bis(*syn*-bis(μ-sulfido)bis(oxomolybdate(V)), (Ph_4P)$_2$-*syn*-[(η^2-CS_3)Mo(O)(μ-S)$_2$Mo(O)(η^2-CS_4)].[20] To a clear orange solution of [Ph_4P]$_2$-*syn*-[(S)Mo(O)(μ-S)$_2$Mo(O)(η^2-S_4)], IX, in CH_3CN, an excess of CS_2 was added. Some ether was added until the two liquid phases were converted to a single liquid phase. After 12 h of stirring, the solution became yellow, and some precipitate had formed. After filtration the addition of ether precipitated the product, which was filtered and washed with ether: FT-IR (KBr pellet, cm^{-1}) νMo=O, 953 (s), νMo–S_b, 466 (m), νMo–η^2-CS_4, (C=S), 979 (m), νMo–η^2-CS_3 (C=S), 1051 (m); FAB^- in magic bullet 876 = P − Ph_4P = P^-, 844 = P^- − S, 800 = P^- − CS_2, 768 = P^- − CS_3. Anal. Calcd for $C_{50}H_{40}P_2Mo_2S_9O_2$: (fw = 1215.2): C, 49.41; H, 3.32. Found: C, 48.70; H, 3.05.

Bis(tetraethylammonium) (η^2-Trithiocarbonato)(η^2-tetrasulfido)-bis(*syn*-bis(μ-sulfido)bis(oxomolybdate(V)), [Et_4N]$_2$-*syn*-[(η^2-CS_3)Mo(O)(μ-S)$_2$Mo(O)(η^2-S_4)], XII. To a solution of $(Et_4N)_2$[(η^2-S_2)Mo(O)(μ-S)$_2$Mo(O)(η^2-S_4)][20] (2 g, 2.7 mmol) in 25 mL of DMF, a solution of Ph_3P (2.9 g, 11 mmol) in 10 mL of DMF was added at once, while stirring. The solution assumed a rose-reddish color and after stirring for about 15 min was diluted with a large excess of ether (~900 mL). Upon standing at −10 °C for 12 h a red oil formed, and the yellow cloudy mother liquor was decanted. The red oil was dissolved in 20 mL of DMF, and an excess of carbon disulfide was added while stirring. After 15 min ether was added to the reaction mixture and precipitated the product as an oil, which soon solidified. The mother liquor was decanted, and the product was recrystallized from CH_3CN/ether and then from DMF/ether, to obtain an orange microcrystalline solid, in excellent yield, 90%: FT-IR (KBr pellet, cm^{-1}) νMo=O, 949 (vs), νMo–S_b, 468 (m), νMo–η^2-S_4 (C=S), 422 (vw), νMo–η^2-CS_3 (C=S), 1058 (vs); UV–vis (DMF solution, 10^{-3} M, nm) 310 (sh), 258 (sh); FAB^- in magic bullet 655 = P^-, 591 = P^- − 2[S], 559 = P^- − 3[S]; ^{13}C NMR in DMSO-d_6 δ = 252 ppm for the CS_3^{2-} ligand. Anal. Calcd for $C_{17}H_{40}N_2Mo_2S_9O_2$ (fw = 784.8): C, 26.01; H, 5.14; N, 3.57; Mo, 24.45; S, 36.77. Found: C, 26.06; H, 5.04; N, 3.54; Mo, 24.73; S, 36.46.

X-ray Diffraction Measurements

(a) Collection of Data. Single crystals of {[(η^2-S_2)Mo(O)(μ-S)$_2$Mo(O)(DMF)$_3$], I, were obtained by vapor diffusion of diethyl ether into a DMF solution of the complex at room temperature. Orange single crystals of [Ph_4P]-*syn*-[(η^2-S_2)Mo(O)(μ-S)$_2$Mo(O)(η^5-C_5H_5)], IV, were obtained by the slow diffusion of diethyl ether into a CH_3CN solution of the complex. Long, thick, needle-like single red crystals of [Ph_4P]$_2$-*syn*-[(S)Mo(O)(μ-S)$_2$Mo(O)(η^2-S_4)], IX, were obtained by the slow diffusion of diethyl ether into a CH_3CN solution of the complex. Orange crystals of [Et_4N]$_4${*syn*-[(S)Mo(O)(μ-S)$_2$Mo(O)(η^2-S_4)]}$_2$, X, were obtained by the slow diffusion of diethyl ether into an acetone solution of the complex.

A single crystal for each complex was carefully chosen and mounted in a thin-walled, sealed capillary tube. Diffraction data for I, IV, IX, and X were collected on a Nicolet P3/F four circle, computer controlled diffractometer at ambient temperature. Graphite monochromatized Mo Kα radiation ($2\theta_{max}$ = 12.50°) was used for data collection and cell dimension measurements (Kα, λ = 0.7107 Å).

Intensity data for all crystals were obtained with use of a θ–2θ step scan technique. Throughout the data collection three standard reflections were monitored every 100 reflections to monitor crystal and instrumental stability. No crystal decay was observed. Accurate cell parameters were obtained from a least-squares fit of the angular settings (2θ, ω, ϕ, χ) of 25 machine-centered reflections with 2θ values between 20° and 30°. Details concerning crystal characteristics and X-ray diffraction methodology are shown in Table I. The raw data obtained were reduced according to a protocol described earlier.[25]

Due to the small μ values (Table I) and the small size of the crystals, no absorption corrections were applied to the data.

(b) Determination of Structures. Three-dimensional Patterson synthesis maps along with the direct methods routine SOLV of the SHELXTL 84 package of crystallographic programs were employed to locate Mo or S atoms. Subsequent difference Fourier maps were used to locate all other non-hydrogen atoms in the asymmetric units.

***syn*-[(η^2-S_2)Mo(O)(μ-S)$_2$Mo(O)(DMF)$_3$], I.** The coordinates of the two molybdenum and four sulfur atoms were determined by direct methods. Subsequent difference Fourier calculations revealed the positions of the remaining non-hydrogen atoms. Isotropic refinement of all non-hydrogen atoms gave an R value of 0.082. All non-hydrogen atoms were assigned anisotropic temperature factors, and the model was refined to a final R value of 0.050. The positions of the hydrogen atoms were calculated and included in the structure factor calculation but were not refined. This inclusion of the H atoms in the structure factor calculation resulted in an R value of 0.037. At this stage all parameter shifts were less than 10% of their estimated standard deviation.

[Ph_4P]-*syn*-[(η^2-S_2)Mo(O)(μ-S)$_2$Mo(O)(η^5-C_5H_5)], IV. The coordinates of the two molybdenum, four sulfur, and the phosphorus atoms were determined by direct methods. The rest of the non-hydrogen atoms were located in successive difference Fourier electron density maps. Least-squares refinement with isotropic temperature factors converged to an R value of 0.093. There is one dianion and one counter cation at general positions per asymmetric unit. All non-hydrogen atoms were refined with anisotropic temperature factors. Refinement converged to an R value of 0.044. The hydrogen atoms, in their calculated positions, were included in the structure factor calculation but were not refined. Final R = 0.038 and R_w = 0.037.

[Ph_4P]$_2$-*syn*-[(S)Mo(O)(μ-S)$_2$Mo(O)(η^2-S_4)], IX. The coordinates of the two molybdenum atoms were determined by direct methods. The rest of the non-hydrogen atoms were located in successive difference Fourier electron density maps. Least-squares

Table I. Summary of Crystal Data, Intensity Collection, and Structure Refinement of $Mo_2(O)_2(\mu\text{-}S)_2\}(\eta^2\text{-}S_2)(DMF)_3$, I, $[Ph_4P][\{Mo_2(O)_2(\mu\text{-}S)_2\}(\eta^2\text{-}S_2)(C_5H_5)]$, IV, $[Ph_4P]_2[\{Mo_2(O)_2(\mu\text{-}S)_2\}(S)(\eta^2\text{-}S_4)]$, IX, and $[Et_4N]_4[Mo_4O_4S_6(S_4)_2]$, X

	I	IV	IX	X
formula	$Mo_2S_4O_5N_3C_9H_{21}$	$Mo_2S_4PO_2C_{29}H_{25}$	$Mo_2S_7P_2O_2C_{48}H_{40}$	$Mo_4S_{14}O_4N_4C_{32}H_{80}$
mw	571.4	756.6	1127.1	1417.6
a, Å	13.152 (3)	11.262 (4)	10.456 (6)	9.261 (2)
b, Å	17.554 (5)	11.688 (4)	12.242 (6)	33.909 (8)
c, Å	17.893 (5)	13.188 (4)	19.785 (7)	10.082 (2)
α, deg	90.00	102.11 (2)	100.50 (3)	90.00
β, deg	90.00	91.73 (3)	78.63 (4)	115.62 (2)
γ, deg	90.00	60.72 (2)	84.62 (4)	90.00
V, Å^3;z	4131;8	1475;2	2408;2	2855;2
d_{calc}, g/cm^3	1.836	1.70	1.55	1.65
d_{obsd},[a] g/cm^3	1.81[a]	1.70[a]	1.56[a]	1.65
space group	*Pcab*	$P\bar{1}$	$P\bar{1}$	$P2_1/m$
cryst dim., mm	0.20 × 0.24 × 1.0	0.13 × 0.42 × 0.44	0.13 × 0.31 × 0.48	0.41 × 0.60 × 1.3
μ, cm^{-1}	15.6	11.4	8.62	13.33
radiation	Mo Kα[b]	Mo Kα[b]	Mo Kα[b]	Mo Kα[b]
data collect.	$2\theta_{max} = 40°$	$2\theta_{max} = 45°$	$2\theta_{max} = 45°$	$2\theta_{max} = 45°$
data used $F_o^2 > 3\sigma(F_o^2)$ parameters	1573[c]	3180	4193	2904
	208	343	551	286
R_c[c]	0.037	0.038	0.065	0.053
R_w[d]	0.039	0.038	0.060	0.053

[a] Obtained by flotation in a $CHBr_3$/pentane mixture. [b] $\lambda = 0.71069$ Å. [c] $R = \sum||F_o| - |F_c||/|F_o|$. [d] $R_w = [\sum w(|F_o| - |F_c|)^2/\sum w|F_o|^2]^{1/2}$. [e] High quality data allowed the use of all intensity data in the refinement of this structure.

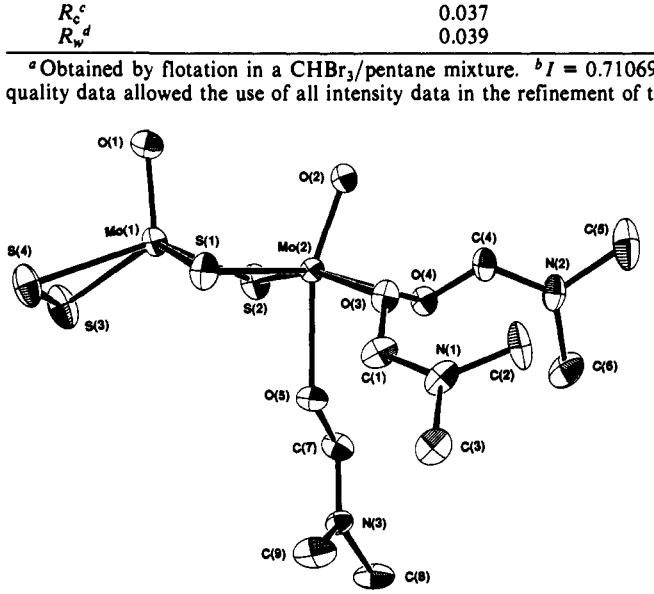

Figure 2. Structure and labeling of the $[(S_2)Mo(O)(\mu\text{-}S)_2Mo(O)(DMF)_3]$ complex, I. Thermal ellipsoids as drawn by ORTEP represent the 40% probability surfaces.

refinement with isotropic temperature factors converged to an R value of 0.116. Assignment of anisotropic temperature factors to all non-hydrogen atoms and subsequent refinement resulted in an R value of 0.069. The hydrogen atoms, in their calculated positions, were included in the structure factor calculation but were not refined. Final $R = 0.065$ and $R_w = 0.060$.

$[Et_4N]_4\{syn\text{-}[(S)Mo(O)(\mu\text{-}S)_2Mo(O)(\eta^2\text{-}S_4)]\}_2$, X. The coordinates of the two molybdenum and five sulfur atoms were determined by direct methods. The rest of the non-hydrogen atoms were located in successive difference Fourier electron density maps. Least-squares refinement with isotropic temperature factors converged to an R value of 0.086. Assignment of anisotropic temperature factors to all non-hydrogen atoms, except for the cation located on the mirror plane, and subsequent refinement resulted in an R value of 0.055. For the cation located on a general position the positions of the hydrogen atoms were calculated, and the latter were included in the structure factor calculations but were not refined. Final $R = 0.053$ and $R_w = 0.053$.

(c) Crystallographic Results. The final atomic positional parameters for *syn*-$[(\eta^2\text{-}S_2)Mo(O)(\mu\text{-}S)_2Mo(O)(DMF)_3]$, I, $[Ph_4P]$-*syn*-$[(\eta^2\text{-}S_2)Mo(O)(\mu\text{-}S)_2Mo(O)(\eta^5\text{-}C_5H_5)]$, IV, $[Ph_4P]_2$-*syn*-$[(S)Mo(O)(\mu\text{-}S)_2Mo(O)(\eta^2\text{-}S_4]$, IX, and $[Et_4N]_4$-$\{syn\text{-}[(S)Mo(O)(\mu\text{-}S)_2Mo(O)(\eta^2\text{-}S_4)]\}_2$, X, with standard deviations have been deposited. Intermolecular distances and angles are given in Table II. The numbering scheme for the anions in I, IV, IX, and X are shown in Figures 2, 3, 4, and 5, respectively.

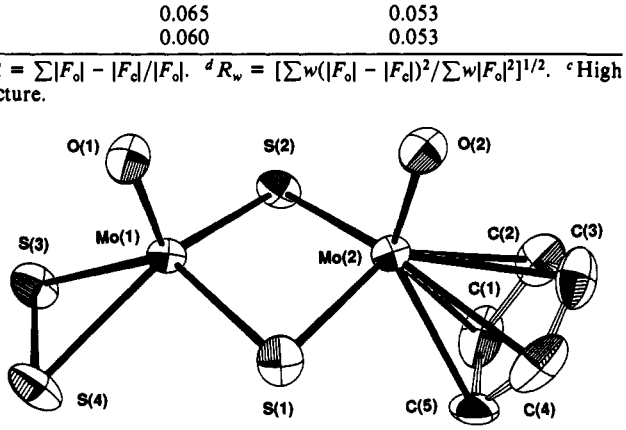

Figure 3. Structure and labeling of the $[(C_5H_5)Mo(O)(\mu\text{-}S)_2Mo(O)(S_2)]^-$ anion in IV. Thermal ellipsoids as drawn by ORTEP represent the 40% probability surfaces.

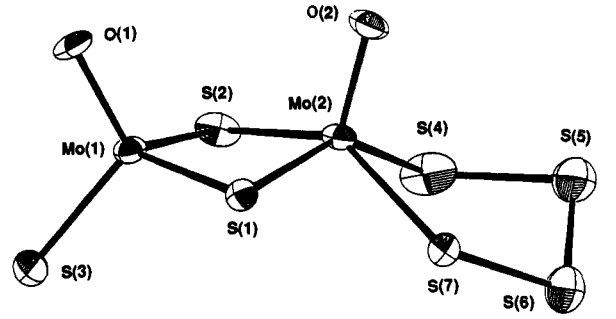

Figure 4. Structure and labeling of the $[(S_4)Mo(O)(\mu_2\text{-}S)_2Mo(O)(S)]^{2-}$ anion in IX. Thermal ellipsoids as drawn by ORTEP represent the 40% probability surfaces.

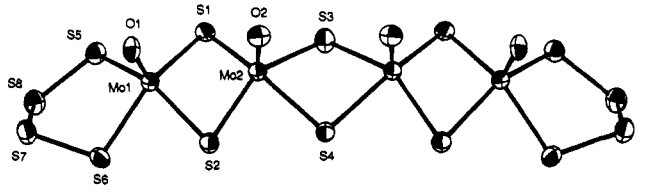

Figure 5. Structure and labeling of the $|[(S_4)Mo(O)(\mu_2\text{-}S)_2Mo(O)(S)]_2|^{4-}$ anion in X. Thermal ellipsoids as drawn by ORTEP represent the 40% probability surfaces.

Synthesis. The sequential oxidative removal of the S_4^{2-} and S_2^{2-} ligands in the $[(S_2)Mo(O)(\mu\text{-}S)_2Mo(O)(S_4)]^{2-}$ anion, by I_2 in DMF solution, proceeds cleanly with formation of the $[(S_2)Mo(O)(\mu\text{-}S)_2Mo(O)(DMF)_3]$, I, and $[(DMF)_3Mo(O)(\mu\text{-}S)_2Mo(O)(DMF)_3]^{2+}$, II, complexes.[20] The substitutional lability

Table II. Summary of Interatomic Distances and Angles for $[Mo_2(O)_2(\mu\text{-}S)_2](\eta^2\text{-}S_2)(DMF)_3$, I, $[Ph_4P][\{Mo_2(O)_2(\mu\text{-}S)_2\}(\eta^2\text{-}S_2)(C_5H_5)]$, IV, $[Ph_4P]_2[\{Mo_2(O)_2(\mu\text{-}S)_2\}(S)(\eta^2\text{-}S_4)]$, IX, and $[Et_4N]_4[Mo_4O_4S_6(S_4)_2]$, X

	I	IV	IX	X
		Distances[a,b]		
Mo–Mo[a]	2.813 (1)	2.855 (1)	2.896 (1)	2.852 (2)
Mo–Mo				3.554 (2)[c]
Mo–S_b	2.317 (4, 3)	2.310 (4, 4)	2.277[d]	2.324[e]
range	2.309 (3)–2.323 (3)	2.306 (2)–2.316 (2)	2.270 (3), 2.285 (3)	2.316 (3), 2.333 (3)
Mo–S_b			2.372[f]	2.350[f]
range			2.360 (3), 2.384 (3)	2.339 (3), 2.362 (3)
Mo–S_b				2.420[c]
range				2.418 (3), 2.421 (3)
Mo–S_L	2.378	2.396	2.412	2.435
range	2.362 (3), 2.395 (3)	2.394 (2), 2.398 (2)	2.405 (3), 2.418 (3)	2.432 (3), 2.438 (4)
Mo=S			2.167 (3)	
Mo=O	1.686	1.673	1.692	1.664
range	1.682 (6), 1.689 (6)	1.660 (4), 1.686 (4)	1.667 (7), 1.717 (6)	1.664 (10), 1.665 (10)
Mo–C (O_L)	2.207 (3, 14)	2.380 (5, 9)		
range	2.186 (6)–2.224 (6)	2.370 (13)–2.399 (8)		
S–S			2.126[g]	2.083[g]
range			2.077 (5), 2.175 (6)	2.070 (5), 2.096 (5)
S–S			1.929 (7)[h]	2.024 (7)[h]
		Angles		
Mo–S_b–Mo	74.77	76.32	77.00	75.19[i]
range	74.39 (1), 74.62 (1)	76.30 (1), 76.34 (1)	76.95 (3), 77.05 (3)	74.83 (3), 75.55 (3)
Mo–S_b–Mo				94.64
range				94.56 (3), 94.72 (3)
S_b–Mo–S_b	102.5	101.3	101.5	98.5[i]
range	102.33 (7), 102.63 (7)	101.12 (8), 101.45 (8)	98.6 (1), 104.3 (1)	97.7 (1), 99.2 (1)
S_b–Mo–S_b				75.8 (1)[c]
S_L–Mo–S_L (interligand)	51.10 (7)	50.72 (9)	86.6 (1)	87.6 (1)
S_L–Mo–O_t	108	109.0	108.3	105.0
range	105.6 (2), 111.3 (2)	108.7 (2), 109.3 (2)	107.1 (3), 109.5 (2)	104.4 (3), 105.8 (3)
S_b–Mo–O_t	106 (4, 2)	107.8 (4, 7)	111.4	109.3 (4, 5)[i]
range	104.1 (2)–110.0 (2)	106.1 (2)–109.3 (2)	110.9 (3), 111.8 (3)	108.1 (3), 109.9 (3)
S_b–Mo–O_t			105.9	105.3[c]
range			104.6 (3), 107.1 (3)	105.0 (3), 105.7 (3)
S_b–Mo–S_t			108.4	
range			108.2 (1), 108.6 (1)	
S_t–Mo–O_t			112.5 (3)	
O_L–Mo–O_L (cis)	77 (3, 1)		79.1 (4, 7)	
range	75.9 (2)–78.2 (2)		78.0 (1)–80.7 (1)	
O_t–Mo–O_L (cis)	88.6		144.4 (4, 19)	
range	88.0 (3), 89.2 (3)		139.7 (1)–148.8 (1)	
O_t–Mo–L_L	160.7 (3)	106.45 (2)	105.5 (4, 12)	

[a] Mean values of crystallographically independent, chemically equivalent, structural parameters. When two numbers are present in parentheses, the first number represents the number of chemically equivalent bond lengths or angles averaged out; the second number represents the larger of the individual standard deviations or the standard deviation from the mean, $\sigma = [\sum_{i=1}^{N}(x_i - \bar{x})^2/N(N-1)]^{1/2}$. [b] In I, for the DMF ligands: The C=O bonds are in the range 1.251 (10)–1.259 (10) Å with a mean value of 1.256 (3, 11) Å. The (O)C–N bonds are in the range 1.311 (12)–1.337 (12) Å with a mean value of 1.322 (3, 12) Å. The N–$(CH_3)_2$ bonds are in the range 1.458 (12)–1.517 (14) Å with a mean value of 1.484 (6, 14) Å. The O–C–N angles are in the range 120 (1)–121.7 (9)° with a mean value of 120.9 (3, 10)°. In IV, the C–C bonds in the C_5H_5 ligand are in the range 1.28 (1)–1.45 (2) Å with a mean of 1.34 (5, 3) Å. For the Ph_4P^+ cation, the P–C bonds are in the range 1.798 (5)–1.801 (5) Å with a mean of 1.800 (4, 5) Å. The C–C bonds are within the range 1.364 (8)–1.411 (7) with a mean value of 1.389 (24, 9). In IX, for cation 1 the P–C bonds are within the range 1.795 (10)–1.809 (10) Å with a mean value of 1.802 (7) with a mean value of 1.389 (24, 9). In IX, for cation 1 the P–C bonds are within the range 1.795 (10)–1.809 (10) Å with a mean value of 1.802 (4, 12). The C–C bonds are within the range 1.33 (2)–1.40 (2) with a mean value of 1.38 (24, 2). For cation 2 the P–C bonds are within the range 1.787 (12)–1.808 (10) Å with a mean value of 1.797 (4, 12). The C–C bonds are within the range 1.33 (2)–1.43 (1) with a mean value of 1.38 (24, 2). In X, for cation N1, N–C range, 1.51 (2)–1.52 (2); mean N–C, 1.52 (4, 2); C–C range, 1.52 (3)–1.53 (2); mean C–C, 1.52 (8, 3); cation N2, N–C range, 1.52 (3)–1.53 (2); mean N–C, 1.53 (4, 3); C–C range, 1.52 (6)–1.53 (6); mean C–C, 1.52 (8, 6). [c] Distances or angles associated with the central Mo–$(\mu_2\text{-}S)_2$–Mo unit. [d] Distances or angles associated with the $MoOS_3$ subunits. [e] Mo(2)–S(1), Mo(2)–S(2). [f] Distances or angles associated with the Mo(O)(S_4) subunits. [g] S–S bonds adjacent to the Mo atoms. [h] Central S–S bond within the S_4^{2-} ligand. [i] Distances or angles associated with the outer Mo–$(\mu_2\text{-}S)_2$–Mo unit.

of the DMF ligands in these complexes makes them ideal starting materials for the synthesis of a multitude of either $[(S_2)Mo(O)(\mu\text{-}S)_2Mo(O)(L]$ or $[(L)Mo(O)(\mu\text{-}S)_2Mo(O)(L)]$ complexes, in simple metatheses reactions.[17] The synthesis of the $[(S_2)Mo(O)(\mu\text{-}S)_2Mo(O)(Cp)]^-$ monoanion as a Et_4N^+, III, or Ph_4P^+, IV, salt is accomplished by the displacement of the DMF ligands in I by the $C_5H_5^-$ anion under anaerobic, moisture free conditions. In a similar ligand substitution reaction the Ph_4P^+ salt of the $[(S_2)Mo(O)(\mu\text{-}S)_2Mo(O)(S_4)]^{2-}$ anion, VIII, can be obtained in pure form and high yield from the reaction of II with Li_2S_4 or $(NH_4)_2S_x$.

The S_2^{2-} ligand in III undergoes both sulfur addition and sulfur abstraction reactions. Sulfur addition to III results in the formation of the $[(S_4)Mo(O)(\mu\text{-}S)_2Mo(O)(Cp)]^-$ complex that in solution exists in equilibrium with III. This equilibrium, shown in simplified form in **1**, has been established by ^1H NMR spectroscopy[21] and almost certainly is affected by $S_n \rightleftharpoons {}^n/_8S_8$ equilibria.

$$[(S_4)Mo(O)(\mu\text{-}S)_2Mo(O)(Cp)]^- + \Delta \rightleftharpoons [(S_2)Mo(O)(\mu\text{-}S)_2Mo(O)(Cp)]^- + {}^2/_8S_8 \quad (1)$$

In previous studies,[2] sulfur abstraction from Mo-coordinated S_x^{2-} ligands by Ph_3P was found to be a facile process for the generation of Mo=S units. In attempts to generate the Mo$(O_t)(S_t)$ chromophore, this reaction has been used effectively in the synthesis of V, IX and X from III, VIII, and $(Et_4N)_2[(S_2)Mo(O)(\mu\text{-}S)_2Mo(O)(S_4)]$, respectively. The reaction of III with a slight excess of triphenylphosphine in either DMF or CH_3CN solution occurs readily and affords V in excellent yield. The solid-state FT-IR spectrum of V shows three absorptions for the Mo=O vibrations at 930, 914, and 903 cm^{-1} and one absorption

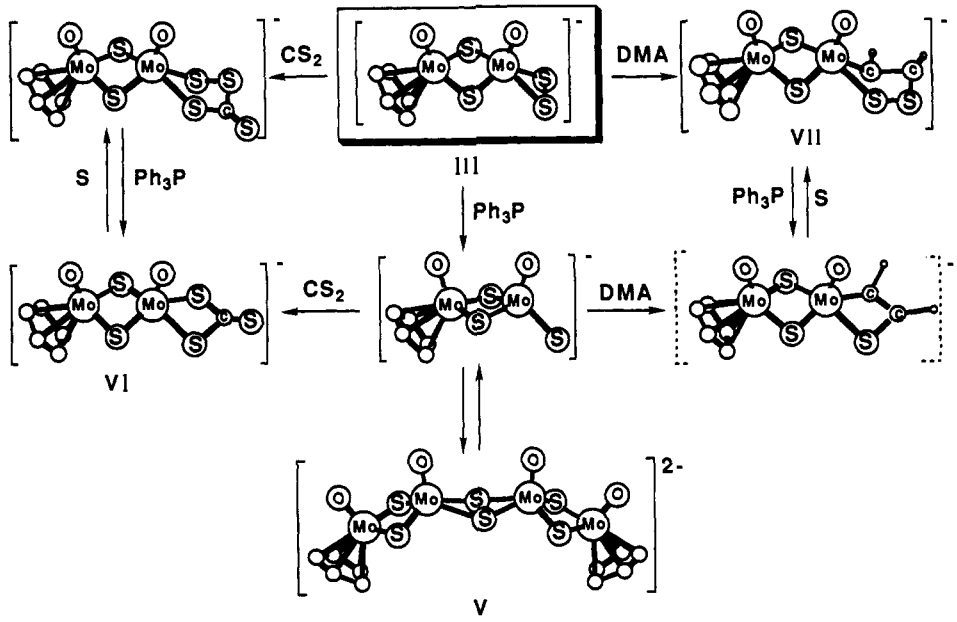

Figure 6. The reactions of the $[(C_5H_5)Mo(O)(\mu\text{-}S)_2Mo(O)(S_2)]^-$ anion with electrophiles. In this figure and also in Figure 7 the structures shown within frames have been determined and are drawn on the basis of crystallographically determined coordinates.

attributed to the Mo–S_b vibration at 464 cm^{-1}. The medium intensity absorption around 500 cm^{-1}, characteristic for the Mo=S functionality, was not observed in the infrared spectrum suggesting that, in the solid state, V very likely contains predominantly a tetrameric dianion that forms as a result of dimerization of the expected $[(S)Mo(O)(\mu\text{-}S)_2Mo(O)(Cp)]^-$ product. Repeated recrystallizations of V did not result in a change of the spectroscopic characteristics of this compound; however, an examination of the electronic spectra as a function of concentration showed a pronounced deviation from the Beer–Lambert law. It appears that both the tetrameric and dimeric forms of V are present in solution at equilibrium.

Evidence for a dimer/tetramer equilibrium also is apparent in the ^{1}H NMR spectra of V. In DMSO-d_6 (vs TMS), V showed two singlets for the Cp resonance: a major one (~90%) at 6.023 ppm and a minor (~10%) at 6.197 ppm. In CD_3CN, the chemical shifts were 6.036 ppm for the major and 6.175 ppm for the minor component, respectively. Total integration of the two Cp^- resonances and comparison with the Et_4N^+ resonances showed the $[Et_4N^+]/[C_5H_5]^-$ ratio = 1. A preliminary study by ^{1}H NMR spectroscopy has shown that for this equilibrium (eq 2) in DMF-d_7 (at 310 K) K_{eq} = ~1 × 10^{-3}.

$$2[(S)Mo(O)(\mu\text{-}S)_2Mo(O)(Cp)]^{2-} \rightleftharpoons [(S)Mo(O)(\mu\text{-}S)_2Mo(O)(Cp)]_2^{4-} \quad (2)$$

The abstraction of sulfur from the Mo-coordinated S_2^{2-} in the anions of the Ph_4P^+ and Et_4N^+ salts of $[(S_2)Mo(O)(\mu\text{-}S)_2Mo(O)(S_4)]^{2-}$ proceeds readily, and the crystalline IX and X can be isolated. In the infrared spectrum of solid IX, vibrations at 890 cm^{-1} (ν-Mo=O) and 494 cm^{-1} (ν-Mo=S) indicate the presence of the $Mo(O_t)(S_t)$ group and suggest a dimeric structure for the $[(S)Mo(O)(\mu\text{-}S)_2Mo(O)(S_4)]^{2-}$ anion. In contrast, spectroscopic features diagnostic for a $Mo(O_t)(S_t)$ chromophore are absent from the IR spectra of X. The latter, in the solid state, has a tetranuclear core structure similar to that proposed for V. The structures of IX and X (vide infra) have been determined, and the anions in these compounds show the core structures anticipated on the basis of their spectroscopic characteristics. The importance of the counterion, in the solid-state isolation of either the dimeric or the tetrameric anions in IX and X, respectively, must be attributed to lattice energies that favor preferential crystallization of either one or the other from an equilibrium mixture (eq 2).

$$2[(S)Mo(O)(\mu\text{-}S)_2Mo(O)(S_4)]^{2-} \rightleftharpoons [(S)Mo(O)(\mu\text{-}S)_2Mo(O)(S_4)]_2^{4-} \quad (3)$$

Spectroscopic evidence for this equilibrium is apparent in the deviation of the electronic spectra of IX and X from the Beer–Lambert law. A dimer–tetramer equilibrium has been reported[26] previously for the $[Mo(L)(\mu\text{-}S)(i\text{-}Bu_2Dtc)]_n$ complexes (L = $NC_6H_4CH_3$, N = 2, 4). Both of the latter were isolated and structurally characterized. In solution these complexes also display deviations from the Beer–Lambert law.

The syntheses of IX and X demonstrate that the abstraction of sulfur by Ph_3P from the $[(S_2)Mo(O)(\mu\text{-}S)_2Mo(O)(S_4)]^{2-}$ anion preferentially occurs at the Mo–η^2-S_2 site. At *ambient temperature*, the Mo–η^2-S_4 site remains unaffected even in the presence of a 4-fold excess of Ph_3P, for an extended period of time (~20 h).

The reactions of V, IX, and X with electrophiles result in dinuclear derivatives that arise by either insertion into the Mo=S_t bond of the dimeric form of the anions or electrophilic attack at the central bridging sulfides in the tetramers followed by bridge cleavage.

Reactions with CS_2. The reaction of V with CS_2 affords the $[Et_4N][(CS_3)Mo(O)(\mu\text{-}S)_2Mo(O)(Cp)]$ complex, VI (Figure 6). This compound was found to be identical with that obtained by sulfur abstraction from $[Et_4N][(CS_4)Mo(O)(\mu\text{-}S)_2Mo(O)(Cp)]$. The latter was obtained by insertion of CS_2 into the Mo–S_2 group in III. The reaction of VI with an excess of sulfur in CH_3CN at 75 °C for 25 h in an open container produced a mixture of $[Et_4N][(S_2)Mo(O)(\mu\text{-}S)_2Mo(O)(Cp)]$ and $[Et_4N][(S_4)Mo(O)(\mu\text{-}S)_2Mo(O)(Cp)]$. This reaction is consistent with the known solution chemistry of other Mo–η^2-CS_3[27] and Mo–η^2-CS_4[10] complexes and involves S addition to the coordinated CS_3^{2-} ligand and CS_2 dissociation from the CS_4^{2-} ligand (eqs 4–6). The reaction

$$[(CS_3)Mo(O)(\mu\text{-}S)_2Mo(O)(Cp)]^- + S \rightarrow [(CS_4)Mo(O)(\mu\text{-}S)_2Mo(O)(Cp)]^- \quad (4)$$

$$[(CS_4)Mo(O)(\mu\text{-}S)_2Mo(O)(Cp)]^- \rightleftharpoons [(S_2)Mo(O)(\mu\text{-}S)_2Mo(O)(Cp)]^- + CS_2 \quad (5)$$

$$[(S_2)Mo(O)(\mu\text{-}S)_2Mo(O)(Cp)]^- + 2S \rightleftharpoons [(S_4)Mo(O)(\mu\text{-}S)_2Mo(O)(Cp)]^- \quad (6)$$

of CS_2 with IX for an extended period of time affords the $[(CS_3)Mo(O)(\mu\text{-}S)_2Mo(O)(CS_4)]^{2-}$ "mixed" ligand complex, XI (Figure 7). The proposed pathway (eqs 7–9) by which XI is obtained can be explained in terms of initial CS_2 insertion into the Mo=S group followed by reactions consistent with the known

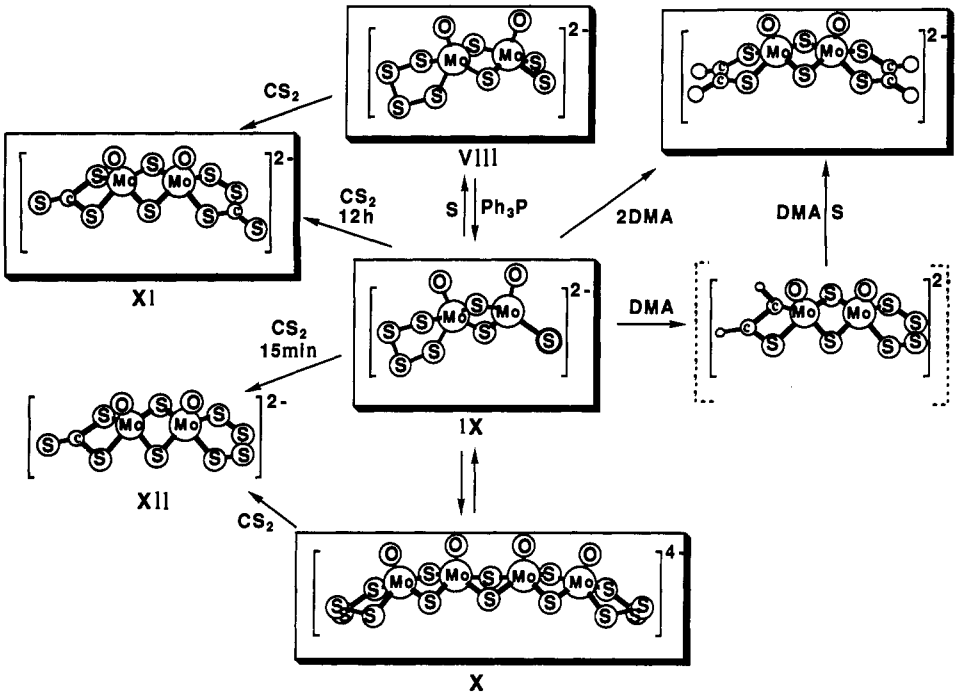

Figure 7. The reactions of the $[(S_4)Mo(O)(\mu_2\text{-}S)_2Mo(O)(S)]^{2-}$ anion with electrophiles.

solution behavior of the Mo–η^2-S_4 and Mo–η^2-S_2 functional groups.[21] The preferential reactivity of the (O)Mo=S group

$$[(S)Mo(O)(\mu\text{-}S)_2Mo(O)(S_4)]^{2-} + CS_2 \rightarrow [(CS_3)Mo(O)(\mu\text{-}S)_2Mo(O)(S_4)]^{2-} \quad (7)$$

$$[(CS_3)Mo(O)(\mu\text{-}S)_2Mo(O)(S_4)]^{2-} \rightleftharpoons [(CS_3)Mo(O)(\mu\text{-}S)_2Mo(O)(S_2)]^{2-} + \tfrac{2}{8}S_8 \quad (8)$$

$$[(CS_3)Mo(O)(\mu\text{-}S)_2Mo(O)(S_2)]^{2-} + CS_2 \rightleftharpoons [(CS_3)Mo(O)(\mu\text{-}S)_2Mo(O)(CS_4)]^{2-} \quad (9)$$

toward CS_2, relative to the (O)Mo–S_4 group (eq 7), is demonstrated by the reaction of CS_2 with X (Figure 7). The latter, obtained in situ by S abstraction from $[(S_2)Mo(O)(\mu\text{-}S)_2Mo(O)(S_4)]^{2-}$, when treated with CS_2 for a short period of time affords only $[(CS_3)Mo(O)(\mu\text{-}S)_2Mo(O)(S_4)]^{2-}$. This complex can be isolated as the Et_4N^+ salt, XII. As discussed previously,[10b] S_2 dissociation from the Mo–η^2-S_4 group in the $[(L_2)Mo(O)(\mu\text{-}S)_2Mo(O)(S_4)]^{2-}$ complexes is influenced by distant effects, due to the equatorial terminal ligands (L) on the second Mo atom. These effects propagate through out-of-plane π bonding and are more pronounced with π donor ligands that include S_4^{2-}, CS_3^{2-}, or Cp^-.

Reactions with 1,2-Dicarbomethoxyacetylene. The reaction of the $[(S_2)Mo(O)(\mu\text{-}S)_2Mo(O)(Cp)]^-$ anions, in either III or IV, with DMA leads to the conversion of the η^2-S_2 ligand into η^2-vinyl disulfide by insertion of DMA into the Mo–S bond of the Mo–η^2-S_2 unit (Figure 6). This reaction is not unexpected and has been reported previously.[28] The vinyl–disulfide complex, $[(\eta^1\text{-}S\text{–}\eta^1\text{-}C\text{–}S_2C_2(COOMe)_2)Mo(O)(\mu\text{-}S)_2Mo(O)(Cp)]^-$, VII, can be converted either thermally or by a sulfur-catalyzed reaction to the corresponding $[(\eta^1\text{-}S\text{–}\eta^1\text{-}C\text{–}S_2C_2(COOMe)_2)Mo(O)(\mu\text{-}S)_2Mo(O)(Cp)]^-$, a 1,2-dithiolene derivative.[21] The ^1H NMR spectrum of VII in CD_3CN solution shows three resonances at 6.15, 3.75, and 3.85 ppm that arise from the $C_5H_5^-$ and the two nonequivalent carbomethoxy groups of the vinyl disulfide ligand, respectively. Addition of 2 equiv of Ph_3P to VII results in sulfur abstraction from the vinyl–disulfide ligand and, gradually and quantitatively, produces a new species which shows three new singlets with chemical shifts at 6.19 ppm for $C_5H_5^-$ and 3.68 and 3.80 ppm for two nonequivalent methyl groups in a 1:1 ratio. These resonances can be attributed tentatively to the vinyl sulfide, $[(\eta^1\text{-}S\text{–}\eta^1\text{-}C\text{–}SC_2(COOMe)_2)Mo(O)(\mu\text{-}S)_2Mo(O)(C)]^-$, complex. Evidence that supports the latter formulation has been obtained by ^1H NMR spectroscopy. Thus, addition of elemental sulfur to the solution that contains the proposed vinyl sulfide complex (Figure 6) results in the total disappearance of the resonances at 6.19, 3.68, and 3.80 ppm (vinyl sulfide complex) and the emergence of resonances at 6.15, 3.75, and 3.85 ppm (vinyl disulfide complex) and 3.76 and 6.20 ppm (dithiolene complex). These results can be rationalized if the coordinated vinyl sulfide ligand undergoes sulfur insertion in either the Mo–S or the Mo–C bonds. Integration of the ^1H NMR signals indicates that insertion into the Mo–C bond is predominant by approximately a factor of three.[21] The observed dithiolene does not arise as a result of the sulfur-catalyzed isomerization of the vinyl disulfide complex. This isomerization reaction, at ambient temperature, is a very slow process. It must be noted that when 2 equiv of Ph_3P were used in the conversion of VII to the vinyl sulfide complex, the conversion was clean and complete. In contrast, when only 1 equiv of Ph_3P was used, in addition to vinyl sulfide, resonances that could be assigned to the dithiolene complex also were detected. The formation of dithiolene in this case is probably due to the slower rate of disappearance of VII that can react further with the vinyl sulfide product to produce dithiolene. This latter reaction has been proposed previously[21] as one of the steps involved in the thermal isomerization of VII to the dithiolene complex.

Upon standing at ambient temperature in solution, the vinyl sulfide complex slowly is converted to a mixture of two species (perhaps isomers) with new resonances at 3.71, 6.29 and 3.69, 6.28 ppm. The yellow crystalline solid isolated from this solution after repeated recrystallizations gave a final product that shows only one set of ^1H NMR resonances at 3.71 and 6.29 ppm. Integration gave a (Cp)/(DMA)/(Et_4N) ratio of 2:1:2.

The ^1H NMR spectrum together with the FT-IR spectrum and elemental analysis[29] are consistent with the formulation $[Et_4N]_2\{[(Cp)Mo_2O_2(\mu\text{-}S)_2]_2[S_2C_2(COOMe)_2]\}$, XIII. The structure of XIII could be that of a tetranuclear linear molecule with the dithiolene ligand serving as a bridge in the center of the

(25) Al-Ahmad, S. A.; Salifoglou, A.; Kanatzidis, M. G.; Dunham, W. R.; Coucouvanis, D. *Inorg. Chem.* **1990**, *29*, 927.
(26) Wall, K. L.; Folting, K.; Huffman, J. C.; Wentworth, R. A. D. *Inorg. Chem.* **1983**, *22*, 2366–2371.
(27) Koo, S.-M. Ph.D. Thesis, University of Michigan, 1990.
(28) Halbert, T. R.; Pan, W. H.; Stiefel, E. I. *J. Am. Chem. Soc.* **1983**, *105*, 5476.
(29) Anal. Calcd for $C_{32}H_{56}N_2Mo_4S_6O_8$ (fw = 1173): C, 32.77; H, 4.81; N, 2.39. Found: C, 33.67; H, 4.40; N, 2.30. FT-IR (KBr disc, cm^{-1}) 956 (s), 914 (m), 466 (m), 1650 (s), 1272 (s), 817 (m), 1709 (m).

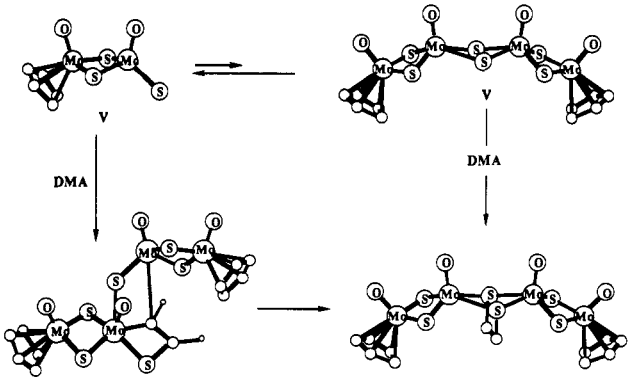

Figure 8. Proposed pathways for the formation of the $\{[(Cp)|Mo_2O_2(\mu\text{-}S)_2]_2[S_2C_2(COOMe)_2]\}^{2-}$ anion.

molecule (Figure 8). The formation of XIII can be envisioned as the result of a coupling reaction between the vinyl sulfide complex and the dimeric form of V. The latter may appear if the vinyl sulfide complex slowly undergoes dissociation of DMA (eqs 10 and 11).

$$[(Cp)Mo(O)(\mu\text{-}S)_2Mo(O)(\eta^1\text{-}S\text{-}\eta^1\text{-}C\text{-}SC_2(COOMe)_2)]^- \rightarrow [(Cp)Mo(O)(\mu\text{-}S)_2Mo(O)(S)]^- + DMA \quad (10)$$

$$[(Cp)Mo(O)(\mu\text{-}S)_2Mo(O)(S)]^- + [(Cp)Mo(O)(\mu\text{-}S)_2Mo(O)(\eta^1\text{-}S\text{-}\eta^1\text{-}C\text{-}SC_2(COOMe)_2)]^- \rightarrow \{[(Cp)Mo_2O_2(\mu\text{-}S)_2]_2[\mu_2\text{-}\eta^4\text{-}S_2C_2(COOMe)_2]\}^{2-} \quad (11)$$

The reaction of $[(Cp)(O)Mo(\mu\text{-}S)_2Mo(O)(S)]_2^{2-}$, V, with excess DMA in CD_3CN solution was monitored by ^1H NMR spectroscopy. A mixture of at least four species was detected. Two of them were identical with those observed previously in the transformation of the vinyl sulfide complex in solution with resonances at 3.71, 6.29 and 3.69, 6.28 ppm. A new, weak, Cp signal at 6.009 ppm also was observed with no apparent DMA signal associated with it. The presence of the dithiolene complex $[(Cp)(O)Mo(\mu\text{-}S)_2Mo(O)(S\text{-}DMA\text{-}S)]^-$ also was evident with resonances at 3.76 and 6.20 ppm. The formation of XIII, in the reaction of V with DMA, very likely follows a pathway similar to the one already described (eq 11, Figure 8).

Upon standing in dimethyl sulfoxide, DMSO, solution for 12 h V undergoes a reaction with the solvent, and a yellow solid can be isolated, XIV. The ^1H NMR of XIV in DMSO-d_6 shows resonances at 6.097 ppm for the Cp ligand and at 2.54 ppm for what appears to be a perturbed DMSO molecule. Integration gives a Cp/DMSO ratio of 2:1. The unperturbed residual DMSO-d_5 (which is always present in the DMSO-d_6 solvent) is observed at 2.50 ppm. The FAB mass spectrum of XIV shows the parent peak with a mass of 977. This mass corresponds to a tetranuclear complex similar to XIII with a DMSO molecule in place of DMA. The formation of XIV may follow a pathway similar to that proposed for the formation of XIII (Figure 8) although the mode of interaction of the DMSO molecule in XIV, albeit symmetric, is not clear.

The reaction of IX with 1 equiv of DMA in CH_3CN for 4 h gives a mixture of products as suggested by ^1H NMR. One hour after mixing, the ^1H NMR spectrum shows free DMA and two singlets at $\delta = 3.826$ and $\delta = 3.743$ ppm, respectively. The signals may be due to the vinyl sulfide ligand that forms by insertion of DMA into the Mo=S bond of IX (Figure 7). At the end of the 4-h period, at least four more peaks appeared. This complexity most likely arises from subsequent reactions associated with the S_4^{2-} ligand. Efforts to isolate the initial vinyl sulfide species have not been successful, and a single product could not be isolated from this reaction. In contrast to the reaction with 1 equiv of DMA, the reaction of IX with more than 2 equiv of DMA in CH_3CN for 12 h with gentle heating gave the expected bisdithiolene $[Ph_4P]_2[(\eta^2\text{-}S_2C_2(COOMe)_2)Mo(O)(\mu\text{-}S)_2Mo(O)(\eta^2\text{-}S_2C_2(COOMe)_2)]$ complex in quantitative yield. The ^1H NMR of this microcrystalline solid in DMSO-d_6 showed only one resonance for the CH_3 groups at $\delta = 3.706$ ppm, nearly identical with that obtained for an "authentic sample"[10b] ($\delta = 3.703$ ppm).

Structure Determinations. *syn*-$[[(\eta^2\text{-}S_2)Mo(O)(\mu\text{-}S)_2Mo(O)(DMF)_3]$, I, and $[Ph_4P]$-*syn*-$[(\eta^2\text{-}S_2)Mo(O)(\mu\text{-}S)_2Mo(O)(\eta^5\text{-}C_5H_5)]$, IV. The structures of the anions in I and IV (Figures 2 and 3) contain as a common structural feature the $[Mo_2(\mu\text{-}S)_2O_2]^{2+}$ core that has been structurally characterized previously in numerous complexes including $[Mo_2O_2S_6]^{2-}$[30] and various $[(L)Mo(O)(\mu\text{-}S)_2Mo(O)(L')]^{n-}$ complexes ($L = L' = [S_2C_2(CO_2CH_3)_2]^{2-}$, dithiolene, $n = 2$;[10b] $L = L' = [S_2C_2(CO_2CH_3)_2]^{2-}$, vinyl disulfide, $n = 2$;[28] $L = S_2^{2-}$, $L' = S_4^{2-}$, $n = 2$;[31] $L = L' =$ histidine, $n = 0$;[32] $L = L' = ox^{2-}$, $n = 2$[33]).

The Mo(1) and Mo(2) atoms in I are elevated from the S(1)S(2)S(3)S(4) and S(1)S(2)O(3)O(4) planes toward the oxo ligands by 0.74 and 0.29 Å, respectively. Similarly the Mo(1) in IV lies 1.05 Å above the S(1)S(2)S(3)S(4) plane. The $(\mu\text{-}S)_2Mo(O)(DMF)_3$ subunit in the structure of I contains the Mo(V) ion in a distorted octahedral coordination with the three DMF ligands arranged facially. As reported previously for the $[Mo_2O_2S_2(C_2O_4)_2(H_2O)_2]^{2-}$[33] and $[Mo_2O_4(C_2O_4)_2(H_2O)_2]^{2-}$[34] complexes, there is only an insignificant trans influence of the terminal oxo group, and the Mo–O_{DMF} distances, in a range from 2.186 (6) to 2.224 (6) Å, are within 3σ of each other (Table II).

In IV, the coordination geometry around the Mo(2) ion can be described as pseudotetrahedral with the η^5-Cp, $=O_t$, and two μ-S ligands occupying the four coordination sites. Individual Mo–S_b distances in each of the two structures (Table II) lie within narrow ranges and indicate that the two Mo atoms in either I or IV are electronically very similar and can be described in terms of a +5 formal oxidation state. The very similar Mo–S_b distances in I and IV at 2.317 (3) and 2.310 (4) Å contrast to the significantly different Mo–Mo distances, Mo–S_b–Mo angles, and the Mo(1)S(1)S(2)–Mo(2)S(1)S(2) dihedral angles within the $[Mo_2(\mu\text{-}S)_2O_2]^{2+}$ cores. The latter, at 151.5° and 163.82° for I and IV, respectively, reflect differences in the Mo–Mo distances (2.813 (1) vs 2.855 (1) Å) and the Mo–S_b–Mo angles (74.8° vs 76.3°). A plausible explanation for this difference is that σ bonding Mo–Mo interactions in IV are weakened by the η^5-Cp ligand coordinated to Mo(2). The onset of σ bonding as a result of Mo–Mo $4d_{x^2-y^2}$ overlap (in a choice of coordinates that places the x and y axes between the equatorial ligands) has been detected by Fenske–Hall MO calculations on the $Mo_2S_4^{2+}$ cores in the $[(L)Mo(S)(\mu\text{-}S)_2Mo(S)(L')]^{n-}$ complexes.[35] This weak σ bonding is suggested to account for the diamagnetic behavior of these complexes without invoking a strong antiferromagnetic coupling mechanism. A Mo–Mo distance comparable to that in IV has been found in the structure of the *syn*-$[MeCpMoO(\mu\text{-}S)]_2$ complex[36] at 2.873 Å. Replacement of the three DMF ligands in I by S_2^{2-} in the structure of the $[(S_2)Mo(O)(\mu\text{-}S)_2Mo(O)(S_2)]^{2-}$ complex[30] shows no significant structural changes in the $[Mo_2(\mu\text{-}S)_2O_2]^{2+}$ core. The Mo–Mo distance, Mo–S_b distances, and Mo–S_b–Mo angles in the $[(S_2)Mo(O)(\mu\text{-}S)_2Mo(O)(S_2)]^{2-}$ complex are found at 2.825 (2) Å, 2.324 (5) Å, and 74.8°, respectively. In the structure of the $[(S_2)Mo(O)(\mu\text{-}S)_2Mo(O)(S_4)]^{2-}$ complex,[31] the introduction of a S_4^{2-} ligand in place of S_2^{2-} results in a core structure with similar Mo–Mo (2.829 (1) Å) and Mo–S_b–Mo angles (74.6 (1), 74.7 (1)°) but unequal Mo–S_b bonds. The latter are separated into two pairs with a "normal" pair (2.316 (3), 2.297 (3) Å) associated with the Mo atom bound to the S_2^{2-} ligand and longer Mo–S_b bonds (2.365 (3), 2.353 (3) Å) found with the Mo

(30) (a) Clegg, W.; Mohan, N.; Muller, A.; Neumann, A.; Rittner, W.; Sheldrick, G. M. *Inorg. Chem.* **1980**, *19*, 2066. (b) Clegg, W.; Sheldrick, G. M.; Garner, C. D.; Christou, G. *Acta Crystallogr.* **1980**, *B36*, 2784.
(31) Hadjikyriacou, A. Ph.D. Thesis, University of Michigan, 1988.
(32) Spivack, B.; Gaughan, A. P.; Dori, Z. *J. Am. Chem. Soc.* **1971**, *93*, 5265.
(33) Armstrong, F. A.; Shibahara, T.; Sykes, A. G. *Inorg. Chem.* **1978**, *17*, 189.
(34) Cotton, F. A.; Morehouse, S. H. *Inorg. Chem.* **1965**, *16*, 2880.
(35) Chandler, T.; Lichtenberger, D. L.; Enemark, J. H. *Inorg. Chem.* **1981**, *20*, 75.
(36) Tanner, L. D.; Haltiwanger, R. C.; Rakowski-DuBois, M. *Inorg. Chem.* **1988**, *27*, 1741–1746.

atom bound to the S_4^{2-} ligand. This lengthening can be attributed to $S_4 \rightarrow Mo$, π bonding (into empty d_{xz}, and d_{yz} orbitals) that strengthens the Mo–S_L bonds and indirectly weakens the Mo–S_b bridge bonds.

$[Ph_4P]_2$-*syn*-[(S)Mo(O)(μ-S)$_2$Mo(O)(η^2-S$_4$)], IX, and $[Et_4N]_4${*syn*-[(S)Mo(O)(μ-S)$_2$Mo(O)(η^2-S$_4$)]$_2$, X. The structure of the $[(S)Mo(O)(\mu\text{-}S)_2Mo(O)(\eta^2\text{-}S_4)]^{2-}$ anion in IX (Figure 4) can be described formally as a square-pyramidal Mo(IV) complex that contains the Mo^{IV}=O unit coordinated by the S_4^{2-} and the $Mo^{VI}OS_3^{2-}$ bidentate ligands. The importance of the Mo^{IV}–Mo^{VI} formalism in the description of the electronic structure of the anion in I finds support in the unequal Mo–S_b bridge bonds in the $[Mo_2(\mu\text{-}S)_2O_2]^{2+}$ core. The short Mo–S_b bridge bonds (2.270 (3), 2.285 (3) Å) found with the $MoOS_3^{2-}$ structural subunit and the significantly longer bonds (2.360 (3), 2.384 (3) Å) found with the MoO(S_4) unit support a structure with appreciable localization of charge. This localization of charge in IX is only partial however as evidenced by the Mo–S bond lengths associated with the S_4^{2-} ligand (2.405 (3), 2.418 (3) Å). These bonds are longer than the Mo^{IV}–S bonds in the $(O{=}Mo^{IV}(S_4)_2]^{2-}$ anion[12] (2.363 (2) and 2.395 (2) Å) and only slightly shorter than the Mo^{V}–S_4 bonds in the $[(S_2)Mo(O)(\mu\text{-}S)_2Mo(O)(S_4)]^{2-}$ complex[31] (2.425 (3) and 2.415 (3) Å). The Mo=S bond in IX, polarized by the proximal =O ligand, at 2.167 (3) Å is appreciably longer than the corresponding Mo=S bond in the Mo(S_t) units in $[Mo_2S_9]^{2-}$ (2.142 (4) Å),[2] $[Mo_2S_7]^{2-}$ (2.141 (4) Å),[2] $[Mo_2S_6]^{2-}$ (2.151 Å),[2] $[Mo_2OS_6]^{2-}$ (2.132 (3) Å),[13] and $[Mo_2OS_8]^{2-}$ (2.135 (7) Å).[13] The Mo–Mo distance in IX at 2.896 (1) Å is significantly longer than those in I, IV, or X.

The structure of the tetraanion in X (Figure 5) consists of two fused $[(S_4)Mo(O)(\mu\text{-}S)_2Mo(O)(S)]^{2-}$ units, similar to those in IX and related by a crystallographic mirror plane. In X, the differences of the Mo–S_b bonds within the outer Mo–(μ-S)$_2$–Mo nonplanar units (dihedral angle, 166.01°) are not as pronounced as those in IX, and the outer Mo–Mo distances are shorter than those in IX (Table II). The two pyramidal Mo atoms, Mo(1) and Mo(2), lie 0.231 and 0.222 Å, respectively, above the S(1)S(2)S(5)S(6) and S(1)S(2)S(3)S(4) planes. The structural data suggest that the mixed-valence description, that weighs heavily in the structural description of IX, is not as important in the structural description of the anion in X. The latter is best described in terms of two, weakly coupled, Mo^{V}–Mo^{V} centers rather than a pair of Mo^{IV}–Mo^{VI} subunits. An outstanding structural feature in X is the unique central Mo–(μ-S)$_2$–Mo rhombic unit. This unit is nonplanar (dihedral angle, 166.04°) and is characterized by unusually long Mo–Mo and Mo–S_b bonds (3.554 (2), 2.420 (3) Å) and oblique Mo–S_b–Mo angles (94.6 (1)°). The apparently weak Mo–S bonds in this central unit of X stem from the localization of electronic charge in IX and account for the pronounced tendency of X toward dissociation.

The effects of $S_{p,d}$–$Mo_{d_{xz},d_{yz}}$ π bonding alluded[11b] to previously for the $[(S_2)Mo(O)(\mu\text{-}S)_2Mo(O)(S_4)]^{2-}$ complex are evident also in the structures of IX and X and are manifested in the alternation of bond lengths within the coordinated S_4^{2-} ligands. An examination of the S–S bond lengths (Table VI) shows longer S–S bonds associated with the Mo bound sulfur atoms and shorter central S–S bonds (S_5–S_6, S_7–S_8). This alternation is a common feature in virtually all of the Mo or W tetrasulfide complexes that have been structurally characterized.[1]

Spectroscopic Properties. Selected features in the infrared and electronic spectra of the complexes are compiled in Table III. In the infrared spectra, the Mo=O stretching vibrations for all complexes appear as strong or medium bands in the region between 890 and 960 cm^{-1}. An examination of structural and spectroscopic data for the (η^5-C_5H_5)Mo(O) group in the $[(L)Mo(O)(\mu\text{-}S)_2Mo(O)(\eta^5\text{-}C_5H_5)]^{-}$ complexes shows the Mo=O vibrations in the lower energy region of the range, between 900 and 909 cm^{-1}. For those of the above complexes that structural data are available (L = S_2^{2-}, SO_4^{2-},[37] $S_2O_3^{2-}$,[37] $C_5H_5^{-}$[36]), the Mo=O bond lengths for the (η^5-C_5H_5)Mo(O) group are comparatively longer than those for the [(L)Mo(O) groups and are found around 1.70 Å. With π donors (L) weaker than η^5-$C_5H_5^{-}$, the ((L))Mo(O) groups (L = S_2^{2-}, CS_3^{2-}, SO_4^{2-},[37] $S_2O_3^{2-}$,[37] S_4^{2-}, CS_4^{2-}) show the Mo=O vibrations at higher energies (~950 cm^{-1}) and somewhat shorter Mo=O distances (~1.67 Å). These effects are consistent with a bonding scheme that utilizes the same Mo d orbitals (d_{xz}, d_{yz}) to simultaneously π bond with the axial oxo ligands and the equatorial ligands (L).

The vibrations associated with the sulfur ligands can be separated within narrow ranges characteristic for each of the ligands. The νMo–S_b vibrations are observed as medium-weak bands between 460 and 469 cm^{-1}. Similarly, the Mo–η^2-S_2 groups show a characteristic medium-strong vibration between 515 and 530 cm^{-1} (probably a S–S stretch). The Mo–η^2-S_4 groups can be identified by the presence of a weak absorption band between 410 and 422 cm^{-1}. A strong vibration in IX at 494 cm^{-1} can be assigned to the Mo=S chromophore. In the IR spectrum of $[(\eta^5\text{-}C_5H_5)Mo(S)(\mu\text{-}S)_2Mo(O)(\eta^5\text{-}C_5H_5)]$ a vibration at 492 cm^{-1} has been assigned previously[36] to the same chromophore.

The electronic spectra of the complexes show absorptions at $\lambda < 460$ nm. A number of these charge-transfer absorptions can be assigned to a particular chromophore. It was revealed, by spectroscopic studies as a function of concentration, that DMF solutions of V, IX, and X do not obey the Beer–Lambert law. Furthermore as the concentration of the complexes was increased the absorption at 270 nm decreased in intensity relative to the absorption around 360 nm in IX and X and the absorption at 320 nm in V. On this basis the 270-nm absorption can be assigned tentatively to the (S)Mo(O) chromophore. The latter is the characteristic feature of the dimeric form of V, IX, and X and prevails in solutions of low complex concentrations. By elimination, the absorptions at 360 nm can be assigned to the (η^2-S_4)Mo(O) chromophores in IX and X, and the absorption at 320 nm in V can be assigned to the (η^5-C_5H_5)Mo(O) unit. Absorptions of similar energies are found (Table III) in the electronic spectra of III, VI, and VII. The latter also contain the (η^5-C_5H_5)Mo(O) unit.

The (O)Mo=S Functional Group. On the basis of the structural details of the $[(S)Mo(O)(\mu\text{-}S)_2Mo(O)(\eta^2\text{-}S_4)]^{2-}$, $[(S)Mo(S)(\mu\text{-}S)_2Mo(S)(\eta^2\text{-}S_4)]^{2-}$,[2] and $[(S)Mo(S)(\mu\text{-}S)_2Mo(O)(\eta^2\text{-}S_4)]^{2-}$[13] complexes we have argued that the MoS_4 and MoS_3O structural subunits in these complexes can be described as containing a significant component of Mo^{VI}, and of the two possible descriptions of the dimers, Mo^{V}–Mo^{V} vs Mo^{IV}–Mo^{VI}, the latter is predominant. The reluctance of the $[(S)Mo(O)(\mu\text{-}S)_2Mo(O)(L)]^{n-}$ complexes to undergo strong coupling indirectly supports the significance of the Mo^{IV}–Mo^{VI} structural description. A Mo^{V}–Mo^{V} dimer would be expected to couple readily and form robust tetramers. As indicated previously, the polarized Mo=S group, in complexes that contain the Mo(O)(S) unit, is a site of considerable reactivity, and dipolar molecules (ROOCC=CCOOR, CS_2, SO_2[37]) readily insert into the Mo=S bond. *The Mo=O bond appears to be relatively inactive in these reactions, and we have no evidence to indicate that this chromophore is directly involved in reactions with electrophilic reagents.*

The importance of the Mo^{VI}(O)(S) group in the chemistry of certain Mo-oxotransferases is well-recognized.[18,38] The extended X-ray absorption fine structure analysis, EXAFS, for the oxidized, active form of xanthine dehydrogenase[39] shows the Mo(VI) coordinated to one oxo group at 1.70 Å, a sulfido group at 2.15 Å, and two additional sulfur atoms at 2.47 Å. Synthetic analogue Mo(VI) complexes that have a comparable Mo(O)(S)(SR)$_2$ coordination sphere are not available. As pointed out previously,[18] species such as $(MoO_2S_2)^{2-}$,[40] $MoOS(R_2NO)_2$,[41] and

(37) Kim, C. G.; Coucouvanis, D. Manuscript in preparation.

(38) (a) Bray, R. C. *Q. Rev. Biophys.* **1988**, *21*, 299. (b) Rajagopalan, K. V. *Biochem. Elem.* **1984**, *3*, 149. (c) Hille, R.; Massey, V. In *Molybdenum Enzymes*; Spiro, T. G., Ed.; Wiley-Interscience: New York, 1985; p 443.

(39) (a) Cramer, S. P. *Adv. Inorg. Bioinorg. Mech.* **1983**, *2*, 259 and references therein. (b) Garner, C. D.; Bristow, S. In *Molybdenum Enzymes*; Spiro, T. G., Ed.; Wiley-Interscience: New York, 1985; p 343.

(40) Muller, A.; Diemann, E.; Jostes, R.; Bogge, H. *Angew. Chem., Int. Ed. Engl.* **1981**, *20*, 934.

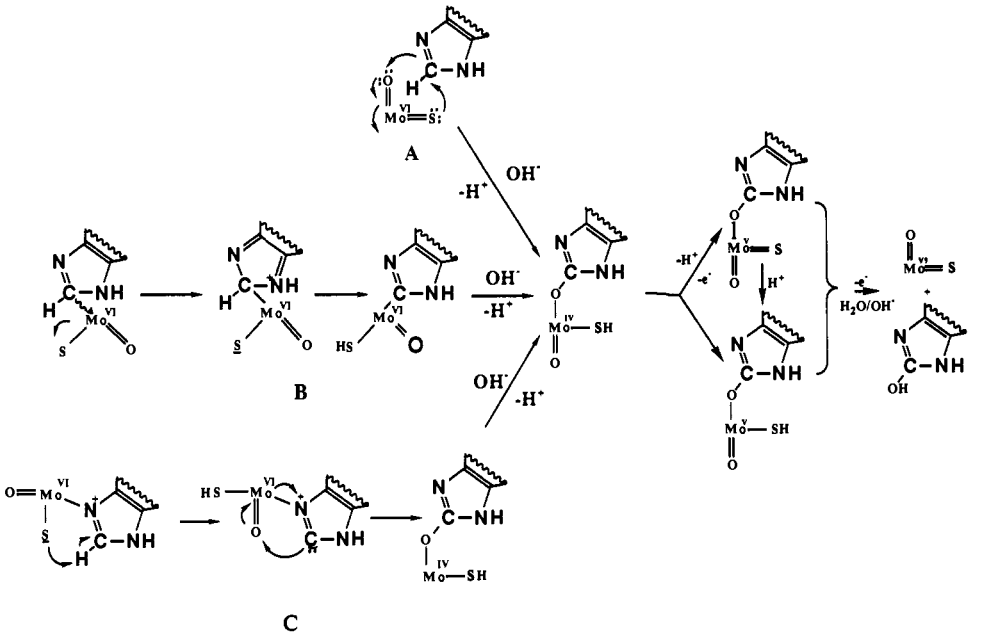

Figure 9. Possible mechanisms suggested for the xanthine oxidase catalyzed oxidation of xanthine to uric acid: (A) a minimal mechanism suggested in ref 18 and (B and C) mechanisms that involve initial attack at the Mo=S bond.

Table III. Infrared, ^{1}H NMR, and Electronic Spectra of I, II, III, and V-XII

compd	νMo-O[a]	νMo-S_b	νMo-S_n[b]	^{1}H NMR[c] (δ)	electronic spectra[d] (nm)
I	948 (s), 954 (s)	469 (m)	527 (m)		269 (br, sh)
II	928 (m), 947 (s)	469 (m)			358 (sh), 286 (br, sh), 276
III	909 (m), 948 (s)[e]	462 (m)[e]	516 (m)	6.113	311, 270
V	903 (s), 914 (m), 930 (s)	464 (m)		6.023 (major),[f] 6.197 (minor)[f] 6.036 (major), 6.175 (minor)	320, 270 (sh)
VI	911 (m), 951 (s)	466 (w)		6.29	313 (sh), 298 (sh), 270 (sh)
VII	906 (m), 944 (s)	464 (w)		3.751 (3 H),[g] 3.846 (3 H),[g] 6.160 (5 H)	462 (br), 395 (br), 298 (sh)[h]
VIII	932 (s), 950 (m)	460 (w)	526 (s), 420 (w)		467 (sh), 360 (sh), 296 (sh), 274 (br)
IX	890 (m), 943 (m)	465 (m)	494 (m), 420 (w)		365, 270
X	933 (s)	462 (m)	410 (w)[i]		365, 270
XI	953 (s)	466 (m)			
XII	949 (vs)	468 (m)	422 (vw)		310 (sh), 258 (sh)

[a] Obtained in KBr discs. [b] n = 1, 2, or 4. [c] Obtained in CH_3CN solution, Cp resonance. [d] Obtained in DMF solution. [e] Obtained in CsI discs. [f] Obtained in DMSO-d^6 solution. [g] Resonances due to the carboalkoxy groups. [h] Obtained in CH_3CN solution. [i] Mo-η^2-S_4.

$Cp^*MoOS(CH_2SiMe_3)$[42] cannot be considered as active site analogues. The $Mo(O)(S)(S_b)_2$ unit in the $[(S)Mo(O)(\mu\text{-}S)_2Mo(O)(S_4)]^{2-}$ complex reported herein shows the Mo=O, Mo=S, and Mo-S_b bond lengths of 1.692 (7), 2.167 (3), and 2.277 (Å), respectively, and at least qualitatively resembles the coordination sphere of the Mo^{VI} in oxidized xanthine dehydrogenase. The dinuclear nature of the $[(S)Mo(O)(\mu\text{-}S)_2Mo(O)(L)]^{n-}$ molecules, the tetrahedral geometry of the $Mo(O)(S)(S_b)_2$ unit, and the rather short Mo-S_b bonds are serious shortcomings. Nevertheless, the $Mo(O)(S)(S_b)_2$ units in these complexes could still enhance our knowledge about the particular reactivity characteristics of the Mo=S/SH groups with the Mo atoms in a somewhat relevant oxidation state and chemical environment. Our studies of the chemical properties of the (O)-Mo^{VI}(S) groups in V, IX, and X clearly show the superior reactivity of the Mo^{VI}=S group relative to the Mo^{VI}=O group and demonstrate the propensity of the Mo=S bond to undergo insertion reactions. These observations, *if applicable to the (O)-Mo^{VI}(S) chromophore in the active site of xanthine dehydrogenase*, support a possible modification of the first step in the proposed[18] minimal mechanism for the oxidation of xanthine to uric acid. In this mechanism the C-8 position of xanthine appears to undergo nucleophilic attack by the Mo=O group to form Mo-O-C, with the Mo=S group serving as a proton acceptor (Figure 9A). As pointed out previously however,[38c] such a mechanism raises an interesting question: "...why replacing the Mo=S with a second Mo=O to give desulfo enzyme should necessarily lead to inactivation of the enzyme,...". This question may be answered if the Mo=O group is not involved in the initial step of the reaction. It is conceivable that xanthine (RH) initially inserts into the Mo^{VI}=S bond by an initial electrophilic attack by the Mo^{VI} at the C-8 position of xanthine. Subsequently the S atom accepts the C-8 proton to form R-Mo^{VI}(O)SH (Figure 9B). An alternate approach could be the initial electrophilic attack by Mo^{VI} at the N-9 position of xanthine followed by the formation of an imidazolium ylide[43] intermediate (Figure 9C). Possible early steps of this new pathway are shown in Figure 9B,C. Subsequent events that may follow include (a) internal $2e^-$ reduction of the Mo and electrophilic attack by R^+ on the Mo=O group and (b) hydroxylation of the Mo(IV) Center to eventually form RO/-Mo^{IV}(O)SH. The remaining steps (Figure 9) toward the formation of uric acid are the same as those proposed earlier.[18]

Not unlike the remarkably reactive μ_2-S (or μ_2-S_2) ligands in the $(CpMo\text{-}\mu\text{-}S)_2S_2$ complexes,[44-47] reactive Mo=S bonds may

(41) (a) Hofer, F.; Holzbach, W.; Wieghardt, K. *Angew. Chem., Int. Ed. Engl.* **1981**, *20*, 282. (b) Wieghardt, K.; Hahn, M.; Weiss, J.; Swiridoff, W. *Z. Anorg. Allg. Chem.* **1981**, *492*, 164. (c) Gheller, S. F.; Hambley, T. W.; Traill, P. R.; Brownlee, R. T. C.; O'Connor, M. J.; Snow, M. R.; Wedd, A. G. *Aust. J. Chem.* **1982**, *35*, 2183.

(42) Faller, J. W.; Ma, Y. *Organometallics* **1989**, *8*, 609.

(43) Gilchrist, T. L. In *Heterocyclic Chemistry*; Pitman Publishing Inc.: Marshfield, MA, 1985; Chapter 7, pp 191-194.

(44) Laurie, J. C. V.; Duncan, L.; Haltiwanger, R. C.; Weberg, R. T.; Rakowski-DuBois, M. *J. Am. Chem. Soc.* **1986**, *108*, 6234.

(45) Casewit, C. J.; Rakowski DuBois, M. *J. Am. Chem. Soc.* **1986**, *108*, 5482.

play an important role as dipolar templates for the activation of substrate molecules. Of particular interest will be reactions with H_2 that may under certain conditions result in heterolytic cleavage of the H_2 bond and formation of the Mo(H)(O)(SH) hydride-hydrosulfide units. In general M(H)(SR) units are rather rare. Notable exceptions include the one present in the [Mo(H)-(tipt)$_3$(PMe$_2$Ph)$_2$] complex[48] (tipt = 2,4,6-SC$_6$H$_2$(^{i}Pr)$_3$) and the Rh(H)(SR) units obtained by the *reversible* addition of H_2 into the Rh-S bonds of the [(triphos)Ru(μ-S)$_2$Rh(triphos)]$^{2+}$ complex.[49] If the Mo(H)(O)(SH) units can be generated, they should be quite reactive, and some of their reactions with disulfides, thiophenes, and thiols may result in S-S or C-S bond cleavage with direct relevance to HDS catalysis.[19,21]

Acknowledgment. The support of this work by a grant from the National Science Foundation (CHE-90006069) is gratefully acknowledged. D.C. also acknowledges stimulating discussions with Prof. W. H. Pearson.

Supplementary Material Available: Tables S1-S3 containing listings of positional parameters, thermal parameters, and selected distances and angles of [Ph$_4$P][(C$_5$H$_5$)Mo(O)(μ-S)$_2$Mo(O)(S$_2$)], IV, (Ph$_4$P)$_2$[(S$_4$)Mo(O)(μ_2-S)$_2$Mo(O)(S)], IX, and (Et$_4$N)$_4$-{[(S$_4$)Mo(O)(μ_2-S)$_2$Mo(O)(S)]$_2$}, X (20 pages); Tables S4-S6 listing structure factors for IV, IX, and X (43 pages). Crystallographic data for the [(DMF)$_3$Mo(O)(μ-S)$_2$Mo(O)(S$_2$)] complex already has been deposited with a previous communication.[20] Ordering information is given on any current masthead page.

(46) Casewit, C. J.; Coons, D. E.; Wright, L. L.; Miller, W. K.; Rakowski DuBois, M. *Organometallics* **1986**, *5*, 951.
(47) Coons, D. E.; Laurie, J. C. V.; Haltiwanger, R. C.; Rakowski DuBois, M. *J. Am. Chem. Soc.* **1987**, *109*, 283.
(48) Burrow, T. E.; Lazarowych, N. J.; Morris, R. H.; Lane, J.; Richards, R. L. *Polyhedron* **1989**, *8*, 1701.
(49) (a) Bianchini, C.; Mealli, C.; Meli, A.; Sabat, M. *Inorg. Chem.* **1986**, *25*, 4617. (b) Bianchini, C.; Meli, A. *Inorg. Chem.* **1987**, *26*, 4268.

Cluster Core Isomerization from Planar to Tetrahedral: Experimental and Theoretical Aspects. Steric Control by the Ligands of Cluster Geometry. Synthesis and Crystal Structure of [Pt$_2$Mo$_2$(η-C$_5$H$_4$CH$_3$)$_2$(CO)$_6$(PCy$_3$)$_2$]

Pierre Braunstein,*,† Claude de Méric de Bellefon,† Salah-Eddine Bouaoud,‡ Daniel Grandjean,§ Jean-François Halet,§ and Jean-Yves Saillard*,§

Contribution from the Laboratoire de Chimie de Coordination, Associé au CNRS (UA 416), Université Louis Pasteur, F-67070 Strasbourg Cédex, France, Département de Chimie, Université de Constantine, Route de Ain-el-Bey, Constantine, Algérie, and Laboratoire de Cristallochimie, Associé au CNRS (UA 254), Université Rennes I, F-35042 Rennes Cédex, France.
Received May 8, 1990

Abstract: The reaction of the phosphine ligands PCy$_3$, P(i-Pr)$_3$, PCyPh$_2$, P(m-Tol)$_3$, P(p-Tol)$_3$ and P(i-Bu)$_3$, with the trinuclear complexes *trans*-[Pt{M(CO)$_3$Cp}$_2$(PhCN)$_2$] (M = Mo, W; Cp = η-C$_5$H$_5$ or Cp′ = η-C$_5$H$_4$CH$_3$) affords the tetranuclear clusters [Pt$_2$M$_2$Cp$_2$(CO)$_6$(PR$_3$)$_2$] (M = Mo, R$_3$ = Cy$_3$, **1**; M = Mo, R$_3$ = Cy$_3$, Cp = Cp′, **2**; M = W, R$_3$ = Cy$_3$, **3**; M = Mo, R$_3$ = (i-Pr)$_3$, **4**; M = W, R$_3$ = (i-Pr)$_3$, **5**; M = Mo, R$_3$ = CyPh$_2$, **6**; M = Mo, R$_3$ = (m-Tol)$_3$, **7**; M = Mo, R$_3$ = (p-Tol)$_3$, **8**; M = Mo, R$_3$ = (i-Bu)$_3$, **9**). Solution studies using ^{31}P NMR spectroscopy have revealed that clusters **1-5** exist as mixtures of two isomers. The geometry of the metallic skeleton is planar triangulated rhombohedral (PTR) in isomers **1a-5a**, like in clusters **6-9**, whereas it is tetrahedral in isomers **1b-5b**. The isomerization process was shown to be reversible, and its thermodynamics has been determined for some of these clusters. The solution ratio of the two structural isomers (i.e., b:a) depends on the solvent used, the temperature, and the steric and electronic properties of the phosphine ligand. Solvents such as toluene and bulky and basic phosphine ligands (e.g., PCy$_3$) favor the tetrahedral isomer b, whereas more polar solvents (e.g., dichloromethane) and small and/or less basic phosphine ligands (e.g., P(p-Tol)$_3$, P(i-Bu)$_3$) point to the planar isomer a. Crystal data for **2b**: monoclinic, space group $P2_1/n$ with $Z = 4$; $a = 10.321$ (3), $b = 24.351$ (8), $c = 21.368$ (6) Å; $\beta = 92.76$ (4)°; $V = 5364$ Å^3; $R = 0.042$, $R_w = 0.052$. Extended Hückel molecular orbital calculations have been carried out on the model compound [Pt$_2$Mo$_2$Cp$_2$(CO)$_6$(PH$_3$)$_2$] in both PTR (a) and tetrahedral (b) geometries. The calculations have shown that, in isomer b, the Mo-Mo σ^* orbital is vacant and the Pt-Pt σ^* one is occupied, while in isomer a Mo-Mo σ^* is occupied and the LUMO has a strong Pt-Pt σ^* antibonding character. They confirmed the equilibrium measurements by revealing the existence of an avoided level crossing between isomers a and b, giving rise to an energy barrier and therefore to two isomers able to coexist in solution.

Introduction

Polyhedral rearrangement is one of the most challenging problems in cluster chemistry.[1] Possible mechanisms for the framework reorganization or isomerization of boranes or carboranes have been proposed already 20 years ago[2a] but are still under current investigation.[2b,c] The conditions for the tetrahedral → butterfly → square-planar transformations of the 20e X_2Y_2 Zintl ions have been recently investigated theoretically.[3] Being more recent, the chemistry of transition-metal clusters has provided only a few examples of *skeletal isomerism*.[4,5] This raises the question

† Laboratoire de Chimie de Coordination, Université Louis Pasteur.
‡ Département de Chimie, Université de Constantine.
§ Laboratoire de Cristallochimie, Université de Rennes 1.

(1) For recent discussions, see: (a) Johnson, B. F. G. *J. Chem. Soc., Chem. Commun.* **1986**, 27. (b) Vahrenkamp, H. *Adv. Organomet. Chem.* **1983**, *22*, 169. (c) King, R. B. *Inorg. Chim. Acta* **1986**, *116*, 99. (d) King, R. B. In *Molecular Structures and Energetics*; Liebman, J. F., Greensberg, J. A., Eds.; Verlag Chemie: Deerfield Beach, FL, 1986; see also references cited therein. For a general review, see: Johnson, B. F. G. In *Transition Metal Clusters*; Johnson, B. F. G., Ed.; Wiley: London, 1980.
(2) (a) Lipscomb, W. N. *Science (Washington, D.C.)* **1966**, *153*, 373. (b) Gimarc, B. M.; Ott, J. J. *Inorg. Chem.* **1986**, *25*, 2708. (c) Wales, D. J.; Stone, A. J. *Inorg. Chem.* **1987**, *26*, 3845.

0002-7863/91/1513-5282$02.50/0